Experimental investigation and mathematical modeling of the mechanical response of hydrogels

Aristeidis A. Papadimitriou, Jérémy H. M. Liely

Department of Mechanical and Manufacturing Engineering, Aalborg University
Fibigerstraede 16, DK-9220 Aalborg East, Denmark
Email: apapad14@student.aau.dk , jliely14@student.aau.dk,

Abstract
Poly(2-hydroxyethyl methacrylate) hydrogels were manufactured via photo-initiated polymerization at various water to monomer concentrations for investigation upon swelling in de-ionized water and salt solution (NaCl). To analyze characteristic features of their behavior, both as-prepared and fully swollen hydrogels were subjected to uniaxial tensile and relaxation tests. Cyclic test with a strain-controlled program is also performed where cyclic loading is interrupted by swelling for analysis of the self-recovery phenomenon of hydrogels. Experimental data are treated as means of appropriate constitutive models to ascertain the effects of composition and degree of swelling (Q) on the visco-elastic response. The constitutive model treats a hydrogel as a two-phase continuum composed of a solid and fluid constituent subjected to swelling under arbitrary deformation with finite strains. Structure-property relations were investigated which allow mechanical properties of the gel to be predicted as function of its composition.

Keywords: pHEMA hydrogels, swelling behavior, mechanical properties, self-recovery, constitutive modeling

1. Introduction

Hydrogels are three-dimensional hydrophilic crosslinked polymers which can extensively swell in a solution medium while maintaining their structure. Dated back to 1950's, hydrogels were invented and patented by D.Lim and O.Wichterle for their potential biological use as soft contact lenses [1].

A variety of chemical compositions can formulate different hydrogels via chemical or physical cross-link junctions [2] and in an array of physical forms; i.e. films, nanoparticles, rods, bars etc. [3]. With respect to this, crosslinked 2-hydroxyethyl methacrylate (HEMA) based hydrogels have attracted a lot of attention for their broad range of applications and technologies to be utilized as bio-materials and specifically, as drug delivery systems [3], hygienic products [4], scaffolds for controlled stem cell differentiation [5, 6], pharmaceuticals [7] and tissue engineering applications [8].

Hydrogels are known to be homogeneous when the critical concentration of water in the monomer mixture is lower or equal to 45%, whereas heterogeneous when the concentration is above this value [9]. Monomer mixture is the solution comprised of the cross-linking agent, initiator and monomer. Heterogeneous hydrogels, also known as sponges due to their porous morphology, constitute of a phase separation at the onset of polymerization induced by the diluent (water). Therefore, understanding key features regarding the physical and mechanical properties of poly-2-hydroxyethyle methacrylate (pHEMA) hydrogels is essential.

During this study, homogeneous and heterogeneous pHEMA hydrogels are synthesized via photo-initiated polymerization in solution in the presence of a free radical initiator and de-ionized water as diluent. The concentration of water to monomer mixture is altered while the water concentration is kept constant. The solvent uptake is investigated by subjecting samples in swelling tests in a similar manner as presented in previous publications [10, 11]. Keeping in mind that the concentration of cross-linking agent in the network alters the swelling behavior of hydrogels, the cross-linking concentration was kept constant while the monomer concentration was modified in order to analyze its effect upon swelling [12]. Swelling of the pHEMA hydrogels is performed both in de-ionized water and salt solution of 1M NaCl by observing alternations in weight measurements over time. The swelling in salt solution is performed to analyse the effect of addition of salt on the swelling properties of pHEMA hydrogels.

Assessment of the effect of swelling is implemented by uniaxial tension, relaxation and multi-cyclic tests

where deformation is interrupted by swelling. The growth of the swelling degree is expected to lead to the decrease of stresses of hydrogels as a function of time and subsequently, to the reduction of the residual strain under retraction. Thus, the hypothesis tested in a previous study by Drozdov et.al. (2014) is further investigated, in which "swelling results in the disappearance of plastic deformation acquired under cyclic pre-loading (self-recovery)" [13]. Considering a hydrogel subjected to uniaxial tension up to its maximum elongation ratio $\kappa_{\max}$ and further unloaded to zero stress, residual strains arise after retraction, characterized by the elongation ratio $\kappa_{\min}$. Self-recovery in hydrogels subjected to cyclic loading, as stated by Sun et.al. (2012) and Drozdov et.al. (2014), is a process in which the swelling of hydrogel results in the reduction of residual strain [13, 14].

The objective of this study is to investigate how the composition of pHEMA hydrogels affects the degree of swelling (Q) and in return their physical and mechanical behavior under uniaxial loading. All experimental data are treated as means of appropriate constitutive models to ascertain the effects of composition and degree of swelling on the visco-plastic and visco-elastic response. Hence, prediction of the mechanical response of HEMA hydrogels as a function of its composition can be achieved.

The constitutive equations utilized in this study for solvent diffusion through by treating a hydrogel as a two-phase continuum and are grounded by the following assumptions : (i) the reference state of an equivalent polymer network (where stresses in chains vanish) coincides with the as-prepared state of a gel but differs from that of a dry undeformed specimen, and (ii) transport of solvent through the polymer network is described by the diffusion equation with the equivalent coefficient of diffusion strongly affected by volume fraction of solid phase. Adjustable parameters in the governing equations are found by fitting experimental data acquired through tensile, relaxation and cyclic tests.

The exposition of the current study is as follows. Section 2 includes the manufacturing process of HEMA gels for each composition. Governing equations of the mathematical model utilized are developed in Section 3. The solvent uptake over a period of time of HEMA-based hydrogels immersed in both de-ionized water and salt solution is presented in Section 4.1. The mechanical response of both as-prepared and fully swollen hydrogels under tension are reported in Section 4.2, while assessment of Q upon the time-dependent response is found in Section 4.3. Investigation of the self-recovery phenomenon of hydrogels through cyclic loading interrupted by swelling is inscribed in Section 4.4. A discussion of the results found in this study is provided in Section 5 and concluding remarks are drawn in Section 6.

2. Experimental

2.1 Materials

All chemicals were purchased from Sigma Aldrich and used as received (without purification), unless otherwise specified. Six series of pHEMA hydrogels were synthesized at various water:monomer-mixture concentrations. 2-hydroxyethyl methacrylate (HEMA) was used as a monomer, di(ethylene glycol) dimethacrylate (DEGDMA) as a crosslinking agent and 2,2-dimethoxy-2-phenylacetophenone (DMPA) as initiator. De-ionised water with a low conductivity ($\approx 0,055$ μS) was used as a solvent during polymerization.

2.2 Specimens preparation

Hydrogels with different compositions, as observed in Table I, were prepared similarly in the following manner. The corresponding grams of HEMA and DEGDMA were dissolved at constant 5.15 g of de-ionised water. Subsequently, DMPA was added into the solution and stirred with a Heidolph MR 3003 Control C magnetic stirrer at 750 rpm for approximately 10 min. Finally the solution was degassed for 10 minutes in an Bandelin Sonorex ultrasound bath at a frequency of 35 kHz for removing air bubbles at room temperature.

Hydrogel specimens were manufactured in three different shapes: (i) cubic specimens of ≈ 2 mm^3, (ii) disks of approximately 2 mm thickness and a diameter of 27 mm and (iii) flat dumbbell specimens for tensile tests (ASTM standard D-638) using a silicon mold under UV irradiation. Both disk and cubic specimens are used only during experimentation of solvent uptake, in order to analyze the effects of the shape upon swelling properties. Polymerization process was performed for 1 hour under argon atmosphere, ensuring the polymerization of the solution's network with a hand held UV Lamp of 6W-Model UVGL-58 and wavelength of 365 nm.

After polymerization as-prepared hydrogels were washed with a water and ethanol mixture, thus removing any excess of un-reacted species, which appeared in the form of a "skin" on the surface of the specimens. Each specimen was weighted on a digital scale with a precision of $\pm$ 1 mg.

During fitting of observations, specimens of disk shape are modeled as thin plates while cubic specimens as spheres. For reasons of statistical quality control, each experimental value noted in this study is the result of three repetitions, unless otherwise stated.

Table. I Sample compositions

Sample no.	HEMA	DEGDMA	DMPA	di-H_2O
1	50 g	1 g	0.51 g	5.15 g
(mol)	(0.38)	(4.1×10^{-3})	(1.99×10^{-3})	(0.29)
2	40 g	0.8 g	0.41 g	5.15 g
	(0.31)	(3.3×10^{-3})	(1.56×10^{-3})	(0.29)
3	30 g	0.6 g	0.31 g	5.15 g
	(0.23)	(2.5×10^{-3})	(1.17×10^{-3})	(0.29)
4	20 g	0.4 g	0.21 g	5.15 g
	(0.15)	(1.65×10^{-3})	(8.19×10^{-4})	(0.29)
5	10 g	0.2 g	0.11 g	5.15 g
	(0.08)	(8.26×10^{-4})	(4.29×10^{-4})	(0.29)
6	5 g	0.1 g	0.01 g	5.15 g
	(0.04)	(4.13×10^{-4})	(3.90×10^{-5})	(0.29)

2.3 Swelling

The swelling kinetics of pHEMA hydrogels were investigated by immersing specimens into de-ionised water and 1M of NaCl solution, at room temperature for at least 72 hours. Before each weight measurement, the sample was wiped with paper to absorb any excess of water on its surface and then placed back into the water bath. The degree of swelling denoted as Q was measured through

$$\mathrm{Q} = \frac{\mathrm{W(t_{sw})} - \mathrm{W_{dry}}}{\mathrm{W_{dry}}} \ \mathrm{(g/g)} \tag{1}$$

where $W(t_{sw})$ denotes the mass of the sample at time t_{sw} and W_{dry} the mass of the dry hydrogel. W_{dry} of the specimens was calculated theoretically by

$$\mathrm{W_{dry}} = \frac{\mathrm{W_{ap}}}{\mathrm{Q_0} + 1} \ \mathrm{(g)} \tag{2}$$

where W_{ap} is the mass of the sample after polymerization and Q_0 denotes the degree of swelling of as-prepared samples in (g/g) (initial degree of swelling).

2.4 Mechanical testing

Different uniaxial tests were conducted on a universal testing machine Instron-5944 equipped with a 2 kN load cell at room temperature. Similarly to the swelling experimentation, each specimen was wiped with paper before measurement and its cross-sectional area was measured using an electronic caliper. The universal testing machine was used to monitor the evolution of the engineering stress σ, which is defined as the ratio of axial force to the cross-sectional area of the undeformed (pre-loaded) specimen. Uniaxial tests performed in this study include (i) tensile deformation, (ii) relaxation and (iii) cyclic deformation using a strain controlled program.

2.4.1 Tensile tests

Tensile tests are used to obtain the rubber elastic behavior of the hydrogel. Generally, tensile testing of hydrogel is performed on a totally immersed sample in a water-bath [15]. However, due to the high cost of including a water-bath to the Instrom-5944 the specimens tensile properties were measured non-immersed. The samples were kept non-immersed for less than 10 minutes due to the substantial evaporation of water. In other study, it has been reported that within 20 minutes, a rigid skin is formed on the lateral surface of the specimens [16]. The rigid skin is to be avoided in order to guarantee the validity of the results. When hydrogel are tested, the water loss during the experiment can significantly influence the mechanical behavior [15]. Tensile tests were performed at a constant strain rate by varying the load, where the strain rate was chosen to be $\dot{\epsilon} = 4.8 \times 10^{-3} s^{-1}$ (cross head speed of 20 mm/min). Since the load deformation characteristics of a specimen depends strongly on its size, to minimize these geometrical factor, load and elongation are normalized respectively to engineering stress σ and engineering strain ϵ. Thus the following equations define σ and ϵ

$$\sigma = \frac{F}{A_0} \tag{3}$$

$$\epsilon = \frac{L_i - L_0}{L_0} = \frac{\Delta l}{L_0} \tag{4}$$

where F is the load, A_0 the initial cross section area, L_i is the instantaneous length and L_0 the initial length of the specimen [17].

2.4.2 Stress Relaxation tests

Stress relaxation is when a constant strain is applied to a specimen and the time dependence of the stress required to maintain that strain is recorded, as seen in Fig. 1. Molecular relaxation processes which take place into the polymer causes the stress to decrease with time. Relaxation modulus $E(t)$ can be defined as

$$E(t) = \frac{\sigma(t)}{\epsilon_0} \tag{5}$$

where $\sigma(t)$ is the time-dependent stress and ϵ_0 the constant strain level [17].

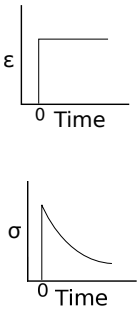

Fig. 1 Stress relaxation, at t=0, a constant strain is applied and the evolution of stress is measured as the time increases [17].

Relaxation tests are performed with an initial strain rate of $\dot{\epsilon} = 4.8 \times 10^{-3} s^{-1}$ up to $\epsilon_0 = 0.3$. It is recommended to proceed relaxation in $t_{rel} = 20$ min (ASTM E-328) but as stated previously, due to the plausible substantial evaporation of water within 20 min, $t_{rel} = 7$ min was used [13].

2.4.3 Cyclic deformation interrupted by swelling

An additional test is performed to relate the swelling properties of pHEMA specimens to their plastic deformation, at which specimens are loaded up to a certain strain, and subsequently unloaded to zero stress. It is believed that hydrogel specimens, during the first loading cycle, are subjected to plastic strain. Subsequently, swelling before the final loading cycle results in a reduction of stresses and residual strain [13, 18]. This phenomenon is commonly refereed to as self recovery and it has been analyzed in other studies [19, 20, 21]. The cyclic test performed is using a strain controlled program where the sample after polymerization is loaded with a strain rate $\dot{\epsilon} = 4.8 \times 10^{-3} s^{-1}$, a maximum strain of $\epsilon_{max} = 0.3$ and a zero minimum stress ($\sigma_{min} = 0MPa$). Specimens are then immersed into a water bath and are allowed to swell until they reach equilibrium Q_{eq}, and loaded again using the same parameters.

2.4.4 Additional experimentation

Any un-reacted products that may exist in the water bath after polymerization are investigated through FTIR analysis with a PerkinElmer Spectrum 100 and UV-scattering on a Varian Cary 50 Bio UV-visible spectrophotometer. FTIR and UV spectroscopy were performed on the water bath after 48 hours of swelling on HEMA-50, 40 and 30 in order to analyze if any un-reacted species from the network diffused into the bath.

3. Mathematical modeling

The present constitutive model was formulated by Drozdov et.al. (2016) in a recently submitted study [22]. Transport of solvent under swelling is considered as the diffusion of water molecules through a gel, which by applying the Flory theory of swelling constitutes another model approach for the kinetics of water uptake. When compared to the linear theory of poroelasticity, constitutive equations provide a small amount of parameters adjustable to experimental data. However, diffusivity of water molecules is not a constant, thus requiring an extra equation describing the increase in coefficient of diffusion which is proportional to the concentration of water molecules.

3.1 Mechanic relations

Hydrogels, as previously mentioned, are regarded as a two-phase medium consisting of a solid (network) and a solvent (water). Although both phases during this study disregard mass exchange in the medium, they are considered however as an inter-penetrating continua; i.e. any elementary volume contains both phases.
Macrodeformation of a hydrogel coincides with that of the polymer network and obeys the molecular incompressibility condition, at which volume deformation is driven only by the changes in water concentration. For an elastic deformation the Cauchy-Green tensors $\mathbf{B}_e$ and $\mathbf{C}_e$ are connected to the macrodeformation tensors $\mathbf{B}$ and $\mathbf{C}$ by

$$\mathbf{B}_{\mathrm{e}} = f^{-\frac{2}{3}}\mathbf{B}, \quad \mathbf{C}_{\mathrm{e}} = f^{-\frac{2}{3}}\mathbf{C} \tag{6}$$

where f is the coefficient of inflation under transition from dry into the as-prepared state. Since the transport of water molecules is modeled as its diffusion through the polymer's network and as previously mentioned, its diffusivity D depends on the concentration c of water molecules in the initial state, hence the flux vector is of the form

$$\mathbf{j} = -\frac{\mathrm{Dc}}{\mathrm{k_B T}}\nabla\mu \tag{7}$$

where D denotes the diffusivity, c is the concentration of water molecules per unit volume in the initial state, k_B is Boltzmann's constant, T is absolute temperature, ∇ is the gradient operator and μ denotes the chemical potential of water molecules. Subsequently combination of Eq. 7 along with the molecular incompressibility condition and the mass conservation law for molecules, results in the equation of diffusion with respect to the deformation gradient **F** for transition from the initial to actual configuration, see Eq. 8.

$$\dot{\mathrm{C}} = \nabla_0 \cdot \left(\frac{\mathrm{DC}}{\mathrm{k_B T}} \mathbf{F}^{-1} \cdot \nabla_0 \mu \cdot \mathbf{F}^{-1} \right) \tag{8}$$

The flux vector **j** is the summation of two vectors, $\mathbf{j}_1$ and $\mathbf{j}_2$ which the former characterizes transport of solvent driven by the inhomogeneity in distribution, while the latter describes permeation of solvent induced by the osmotic pressure's gradient. This results in two limiting cases: (i) when degree of swelling is small (Q«1) the flux vector transforms into the Fick's law, whereas if its high (Q»1) then it is equivalent to Darcy's law. It follows, that the boundary condition at the interface between a gel and an aqueous solution is

$$\ln \frac{\mathrm{Cu}}{1+\mathrm{Cu}} + \frac{1}{1+\mathrm{Cu}} + \frac{\chi}{(1+\mathrm{Cu})^2} + \frac{\Pi \mathrm{u}}{\mathrm{k_B T}} = 0 \tag{9}$$

where *u* stands for the volume occupied by a water molecule, χ is the Flory-Huggins parameter; i.e. regards for interactions between water molecules and chain segments and Π stands for the Lagrange multiplier arose from the molecular incompressibility condition.

For an elastic network and a solvent, transport of water molecules within the continuum theory of mixtures is described by Eq. 10, in which ζ denotes coefficient of friction between water molecules and segments of chains, $\mathbf{v}_w - \mathbf{v}_n$ the relative velocity and ϕ_w the volume fraction of water molecules.

$$\zeta(\mathbf{v}_\mathrm{w} - \mathbf{v}_\mathrm{n}) = -\phi_\mathrm{w} \nabla \Pi \tag{10}$$

3.2 Governing equations

Constitutive equations of the model are developed by means of the free energy imbalance inequality and involve equations of continuum theory of mixtures, chemical potential of water molecules, strain energy density (assuming an incompressible neo-Hookean material) and stress-strain relations (Cauchy stress and rate-of-strain tensors).

Helmholtz free energy of a hydrogel per unit volume in the initial configuration Ψ is defined as the sum of energy of water molecules disregarding interactions with the solid phase Ψ_1, energy of network not interacting with water Ψ_2 and energy of mixing Ψ_3. Differentiation of Helmholtz free energy with respect to time leads to

$$\dot{\Psi} = \mathrm{K}\dot{\mathrm{C}} + 2\mathbf{K}_\mathrm{e} : \mathrm{D} \tag{11}$$

During this study spherical and thin film hydrogel specimens were manufactured by photo-initiated polymerization in solution. In the following sections, governing equations are presented along with their corresponding boundary conditions for both shapes. A more comprehensive review of the governing equations and their derivation are enclosed in a recently submitted study by Drozdov et.al. (2016) [22].

3.2.1 Sphere swelling

Assuming a spherical gel particle occupies a domain (Ω) in a three-dimensional space ($0 \leq \Omega \leq 2\pi$) and symmetric swelling induced deformation, the governing equations in the new notation are described by

$$\frac{\partial Q}{\partial t} = \frac{\partial}{\partial x}\Bigg(x^{\frac{1}{3}} (1+Q)^{\beta-2} \Bigg\{ 3x \Bigg[\left(\frac{1+(1-2\chi)Q}{(1+Q)^3} + \frac{gQ}{(1+Q)^2} \right) \left(\frac{F}{x} \right)^{\frac{4}{3}} + \frac{gQ}{(1+Q_0)^{\frac{2}{3}}} \Bigg] \frac{\partial Q}{\partial x} - \frac{2gQ}{(1+Q_0)^{\frac{2}{3}}} \frac{F}{x} \left((1+Q)\frac{x}{F} - 1 \right)^2 \Bigg\} \Bigg) \tag{12}$$

and

$$\ln \frac{\mathrm{q}}{1+\mathrm{q}} + \frac{1}{1+\mathrm{q}} + \frac{\chi}{(1+\mathrm{q})^2} + \frac{\mathrm{g}}{1+\mathrm{q}} \left(\frac{(1+\mathrm{q})^2}{(1+\mathrm{Q_0})^{\frac{2}{3}} (\mathrm{F}|_{\mathrm{x}=1})^{\frac{4}{3}}} \right) = 0 \tag{13}$$

where Q_0 denotes the degree of swelling in the as-prepared state, g is the dimensionless elastic modulus ($g = \frac{Gu}{k_B T}$) and the average degree of swelling for spherical specimens is found to be

$$\bar{Q} = \frac{1}{U_0} \int_0^{Q_0} Q \, dU = F|_{x=1} - 1 \tag{14}$$

The corresponding boundary conditions to the above governing equations include

$$Q|_{t=0} = Q_0,\ \frac{\partial Q}{\partial x}|_{x=0} = 0,\ Q|_{x=1} = q$$
$$\frac{\partial F}{\partial x} = 1 + Q,\ F|_{x=0} = 0$$

Diffusivity of solvent molecules in a spherical hydrogel was found to be

$$D_0^{sphere} = \frac{{R_0'}^2 K}{3(1+Q_0)^{\frac{2}{3}}} \tag{15}$$

where R_0' denotes the radius of the as-prepared specimen and K is a parameter in the model which minimizes inconsistencies between experimental data and simulation results.

3.2.2 Thin film swelling

Considering a thin film specimen occupying the domain Φ with a thickness t much smaller than any other dimensions of the sample ($\mathrm{t_{film}} << \mathrm{length, width}$) and allowing unconstrained swelling; i.e. sample is considered to be immersed in a solvent and not connected to any substrate, the governing equations are given by

$$\frac{\partial Q}{\partial t} = \frac{1}{F(1+Q_0)^{\frac{4}{3}}}\frac{\partial}{\partial x}\left((1+Q)^{\beta-2}\left[\frac{1+(1-2\chi)Q}{(1+Q)^3} + gQ\left(\frac{F}{(1+Q_0)^{\frac{2}{3}}} + \frac{1}{(1+Q)^2}\right)\right]\frac{\partial Q}{\partial x}\right) \tag{16}$$

and

$$\ln\frac{\mathrm{q}}{1+\mathrm{q}} + \frac{1}{1+\mathrm{q}} + \frac{\chi}{(1+\mathrm{q})^2} + \frac{\mathrm{g}}{1+\mathrm{q}}\left(\frac{\mathrm{F}(1+\mathrm{q})^2}{(1+\mathrm{Q_0})} - 1\right) = 0 \tag{17}$$

The corresponding boundary conditions to the above governing equations include

$$Q|_{t=0} = Q_0,\ \frac{\partial Q}{\partial x}|_{x=0} = 0,\ Q|_{x=1} = q$$
$$F = \left(\frac{\int_0^1 (1+Q)^{-1}\,dx}{\int_0^1 (1+Q)\,dx}\right)^{\frac{2}{3}}$$

Diffusivity of solvent molecules in a thin film is calculated by

$$D_0^{film} = \frac{H_{ap}^2 K}{4(1+Q_0)^2}. \tag{18}$$

where H_{ap} denotes the thickness of as-prepared specimens.

4. Results

4.1 Swelling in de-ionized water and salt solution

Solvent uptake of HEMA hydrogels prepared via photo-initiated polymerization in solution at various concentrations of water:monomer-mixture was investigated. Observations of swelling in water and in 1M of NaCl solution are depicted in Fig. 2 and 3, respectively.
The initial degree of swelling of all samples, as previously explained is theoretically determined from Eq. 2 and can be observed in Table II. It is noted that swelling in de-ionized water was performed for both spherical and thin plate (disc) specimens while swelling in 1M NaCl solution was performed only for thin plate specimens. Spherical samples are prepared for only one composition; i.e. that of HEMA-10 (see Table I).

4.1.1 Experimental swelling

Fig. 2 reveals that the swelling degree of each specimen at time t_i; i.e. i is the i^{th} value, is monotonically increased relatively to initial swelling until equilibrium. The evolution of swelling for each thin plate specimen appears identical due to their similar shape, contrary to the spherical samples. Equilibrium degree of swelling is reached for all thin plate samples after 24 hrs, except spheres for which is reached after 7 hrs. Highest equilibrium degree of swelling is observed for HEMA 5 with Q_{eq}= 0.85 g/g (see Fig. A.7 in Appendix A), whereas the lowest is observed for HEMA 50 with Q_{eq}= 0.48 g/g. This difference arises from the variation

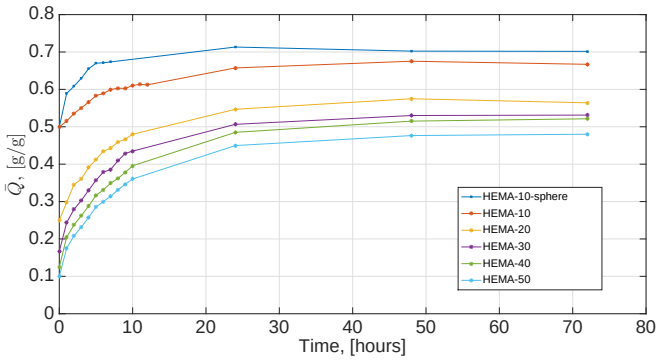

Fig. 2 Swelling degree over time for each series in water.

of water to monomer concentration in each series. By decreasing the concentration of monomer in the network, a higher amount of solvent is able to diffuse through the network leading to a less dense network and thus increasing the equilibrium degree of swelling. Additionally, it is observed that the swelling behavior of HEMA-50 is in quantitative agreement with previous studies of Drozdov et.al. (2015) and Lee and Buchnall (2008) [10, 13].

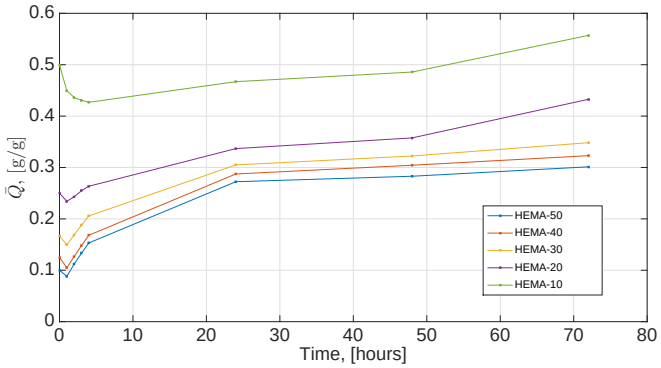

Fig. 3 Swelling degree over time for each series in salt solution.

Observation of swelling in 1M NaCl bath illustrate a reduction in Q_{eq} between 10 to 20 $\%$ when compared to samples in water bath as illustrated in Fig. 3. This is in good agreement with Ting and Jeng Huang (2014), at which during their study they performed an identical experiment on HEMA gels in which immersion in 1M of NaCl solution resulted in a decrease of Q_{eq} of approximately 20 $\%$ in comparison to Q_{eq} in water [23]. Highest degree of swelling is reported to be for HEMA-10 with $\bar{Q} \approx 0.56$ g/g, followed by a HEMA-20 at $\bar{Q} \approx 0.43$, while the remaining samples show an almost identical swelling behavior with $\bar{Q}$ located between 0.3-0.35. All samples indicate a weight decrease during the first hour of measurement followed by a gradual increase, whereas HEMA-10 decreases constantly up to 5 hrs. This seems to contradict the overshooting effect of gels ;i.e. initial swelling up to a maximum point followed by a decrease until equilibrium [24, 25]. However, the overshooting effect has been observed on stimuli-responsive hydrogels in an acidic medium at which thus far there is no universal explanation due to different gel systems and parameters (temperature, pH, cross-linking degree, etc). Additionally, all hydrogels have an increase in $\bar{Q}$ above their initial degree of swelling after approximately 3 hrs except HEMA-10 which increases after 50 hrs. It is in the authors belief that as-prepared hydrogels contain de-ionised water initially in their network, at which an exchange between de-ionised water and salt occurs when immersed in a salt solution, thus affecting the swelling behavior.

Table. II Swelling degree of specimens after polymerization.

Sample series	Initial swelling (g/g)	Weight difference (%)
HEMA-50	0.09998	-0.62
HEMA-40	0.12497	-0.06
HEMA-30	0.16661	1.53
HEMA-20	0.24988	2.37
HEMA-10	0.49952	5.59
HEMA-5	0.99980	7.15

An additional drying experiment was performed to verify if the expected dry mass (theoretically determined) was similar to the real dry mass (experimentally determined). Table II indicates a small variance between experimental and expected weight of hydrogel samples. During this experiment, the weight of as-prepared hydrogels was measured before and after samples were placed in a vacuum oven at 50°C for a week. Although weight differences for hydrogels at monomer concentrations of 50, 40 and 30 did not exceed 1.5%, the difference in weight are attributed to the possible remaining water trapped in the hydrogel network. It is noted that the negative values represent a higher expected weight than experimental.

4.1.2 Fitting of observations

Parameters of the constitutive equations, see Eq. 16-18, including the Florry-Huggins parameter χ, dimensionless elastic modulus g and diffusivity D_0 have been determined by matching experimental data to best fit the mathematical model and can be seen in Table III. Fig. 4-6 display experimental and simulation data, at which swelling boundaries Q_{eq} and Q_0 were determined for each composition in Fig. 2. As previously stated, the material coefficient K is chosen in order to reduce any inconsistencies between model and experimental data. In Fig. 7 the swelling response of spherical HEMA-10 samples is depicted, at which both HEMA-10-1 and 2 are the raw experimental data of one sample. Fig. 6B it can be seen that HEMA-5, when immersed into water, is subjected to shrinking from a swelling degree Q_0 = 1 g/g to Q_{eq}= 0.85 g/g, nevertheless the swelling kinetics appear to be similar to disks.

4.2 Tensile tests on as-prepared and fully swollen hydrogels

The stress-strain curves for as-prepared and fully swollen specimens loaded up to breakage, are depicted in Fig. 8 and 9 respectively. Fig. 10 represents the fitting of experimental data for tension on swollen specimens.

Table. III Material parameters of HEMA hydrogels.

Sample series	Q_0	Q_{eq}	ρ_i $\times 10^{-3}$	g	χ $\times 10^{-6}$ (cm^2/s)	D_0 $\times 10^{-3}$	K
HEMA-50	0.10	0.48	0.9091	3.55	0.985	5.87	0.71
HEMA-40	0.12	0.52	0.8889	3.37	0.956	5.61	0.71
HEMA-30	0.17	0.53	0.8572	3.18	0.949	5.22	0.71
HEMA-20	0.25	0.56	0.8001	3.55	0.930	4.54	0.71
HEMA-10	0.50	0.67	0.6669	2.61	0.878	4.89	1.10
HEMA-5	1.00	0.85	0.4981	2.58	0.798	6.75	2.70
HEMA-10-sphere-1	0.50	0.72	0.6669	2.61	0.853	4.91	6.50
HEMA-10-sphere-2	0.50	0.69	0.6669	2.61	0.864	4.70	6.0

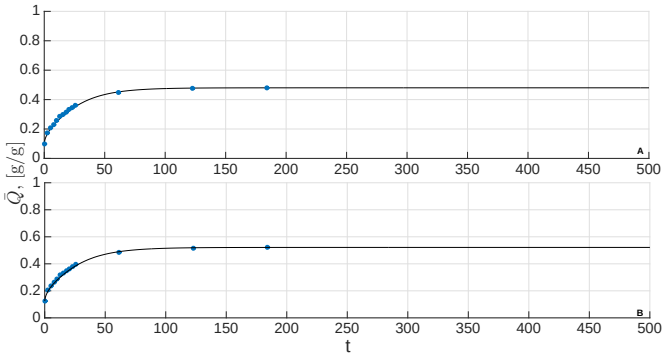

Fig. 4 Average degree of swelling $\bar{Q}$ versus dimensionless time t. Circles: experimental data of discs with thickness 2 mm. Solid lines: simulation data. A: HEMA-50, D_0= 5.87 $\cdot 10^{-6}$ cm^2/s. B: HEMA-40, D_0= 5.61 $\cdot 10^{-6}$ cm^2/s.

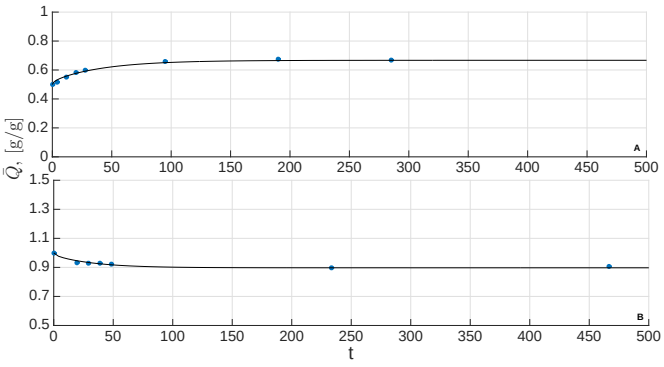

Fig. 6 Average degree of swelling $\bar{Q}$ versus dimensionless time t. Circles: experimental data of discs with thickness 2 mm. Solid lines: simulation data. A: HEMA 10, D_0= 4.89 $\cdot 10^{-6}$ cm^2/s. B: HEMA 5, D_0= 6.75 $\cdot 10^{-6}$ cm^2/s.

As-prepared specimens HEMA-50:30 display a visco-elastic response with a maximum stress located at the yielding point (≈4.5 % of strain), whereas HEMA-20 illustrates a constant stress after 5% of strain, with no indications of a yielding point. Furthermore, HEMA-10 and HEMA-5 display a visco-elastic response with a linear increase of stresses up to breakage.

As-prepared samples of HEMA-50 and 40 differ slightly in their stress-strain response when compared to the remaining samples. Although good reproducibility of the uniaxial tensile test was observed, strain at breakage deviate profoundly for each sample. Specifically, as-prepared specimens lie in the interval between 35 and 180 % of strain, whereas fully swollen specimens are located between 40 and 95 % of strain.

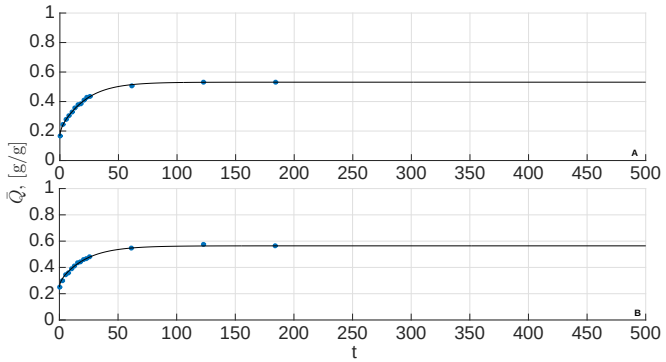

Fig. 5 Average degree of swelling $\bar{Q}$ versus dimensionless time t. Circles: experimental data of discs with thickness 2 mm. Solid lines: simulation data. A: HEMA-30, D_0= 5.22 $\cdot 10^{-6}$ cm^2/s. B: HEMA-20, D_0= 4.54 $\cdot 10^{-6}$ cm^2/s.

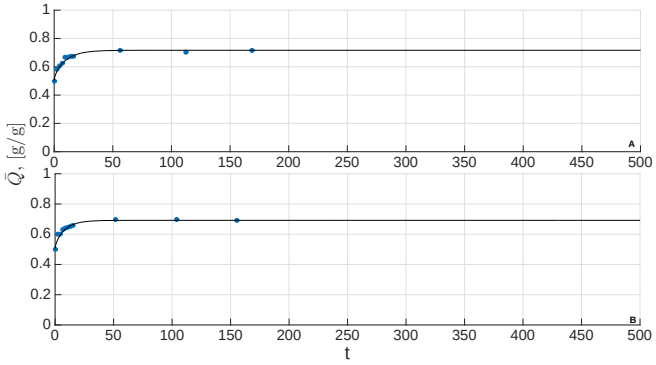

Fig. 7 Average degree of swelling $\bar{Q}$ versus dimensionless time t. Circles: experimental data of spheres with different radium R_0'. Solid lines: simulation data. A: HEMA 10,R_0'= 1.72 mm, D_0= 4.91 $\cdot 10^{-6}$ cm^2/s. B: HEMA 10, R_0'= 1.75 mm, D_0= 4.7 $\cdot 10^{-6}$ cm^2/s.

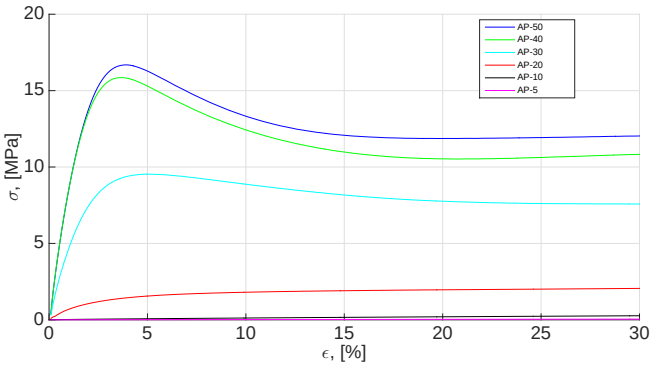

Fig. 8 Stress σ versus strain ϵ for as-prepared specimens.

Stress is considerably reduced while the degree of swelling is increasing, at which the maximum stress observed was for HEMA-50 ($\approx$ 16.5 MPa) and the lowest was for HEMA-5 ($\approx$ 0.2MPa). For fully swollen and as-prepared specimens, a decrease in monomer concentration tends to an increase of swelling degree and subsequently to a decrease of stresses.

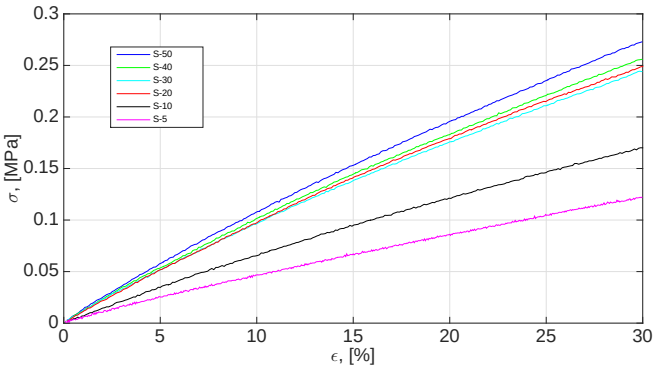

Fig. 9 Stress σ versus strain ϵ for fully swollen specimens.

Elastic modulus G obtained by fitting of experimental data, is used to calculate the coefficient G_1 using the least square method.

$$G_1 = \frac{G}{(1+Q_{eq})^{\frac{1}{3}}(1+Q_0)^{\frac{2}{3}}},\ \sigma = G_1(\lambda - \lambda^{-2}) \quad (19)$$

where λ denotes elongation.

4.2.1 Effect of composition on material properties

Evolution of diffusivity and elastic modulus for cross-linked HEMA hydrogels as a function of the monomer mass fraction are displayed in Fig. 11 and 12, respectively. The monomer mass fraction ρ_i describes the mass ratio of the monomer mixture (HEMA, DEGDMA and DMPA) over the total amount of species in the network, including water.

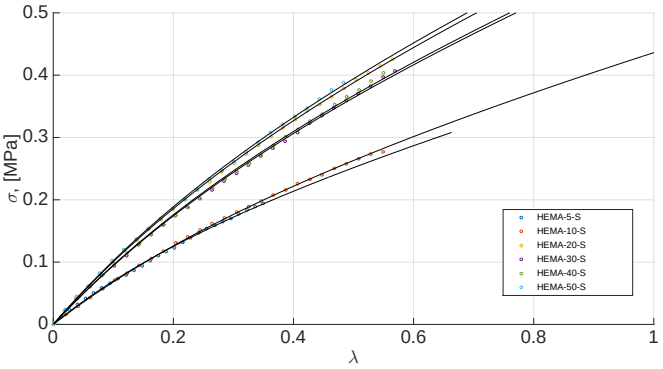

Fig. 10 Stress σ versus elongation ratio λ for as-prepared. Solid lines: approximation of the data using Eq. 19.

Diffusivity displays a linear decrease between the first four hydrogel compositions (HEMA-50:20) followed by a rapid increase for the remaining series. The initial decrease was expected due to the lowering of the initial degree of swelling, while K and H_{ap} are kept constant, as can be seen in Eq. 18. The highest diffusivity (D_0 = 6.75 $\times 10^{-6}$ (cm^2/s)) is reported for HEMA-5 having a mass fraction of approximately ρ_i = 0.5, while the lowest is observed for HEMA-20 (D_0 = 4.54 $\times 10^{-6}$ (cm^2/s)) with a ρ_i = 0.8.

Elastic modulus is displayed in Fig. 12 which was determined by best fitting of the elastic region of the stress-strain curve. Modulus of elasticity for as-prepared specimens displays somewhat a relative decrease with regards to mass fraction. The difference between HEMA-50 and HEMA-40 series might be attributed to experimental errors and poor reproducibility of their tensile response with a reported maximum standard deviation equal to 2.55.

Fully swollen specimens on the other hand, exhibit a linear relation of elastic modulus with respect to the

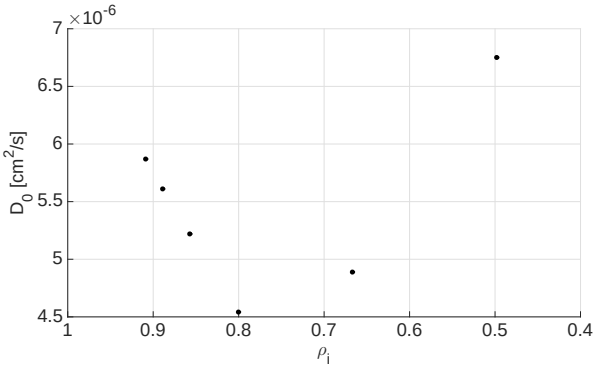

Fig. 11 Evolution of diffusivity of HEMA hydrogels with respect to mass fraction.

mass fraction of monomer mixture. Specifically, a linear decrease is observed at which the greatest modulus (G = 0.39 MPa) is achieved for HEMA-50, while the lowest (G = 0.18 MPa) for HEMA-5.

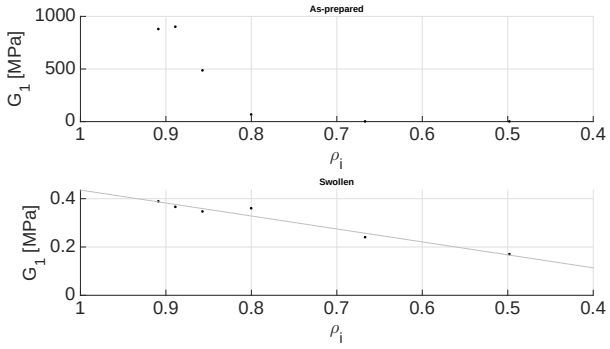

Fig. 12 Evolution of elastic modulus of HEMA hydrogels with respect to mass fraction.

4.3 Relaxation tests on as-prepared and fully swollen hydrogels

Effects of swelling on time dependent response was conducted by uniaxial tension on hydrogel specimens up to ϵ = 0.3 during a relaxation period of 7 minutes as seen in Fig. 13 and 14.

As-prepared specimens displayed a stress relaxation for all except HEMA-10, while fully swollen specimens indicated no signs of relaxation. This may indicate that an intermediate region exists at which relaxation disappears. For this reason, an additional experiment was performed in which samples were swollen at various swelling degrees and then subjected to relaxation. Through this experiment, the swelling degree at which the specimens indicate no more relaxation was determined to lie between 40-45 % swelling.

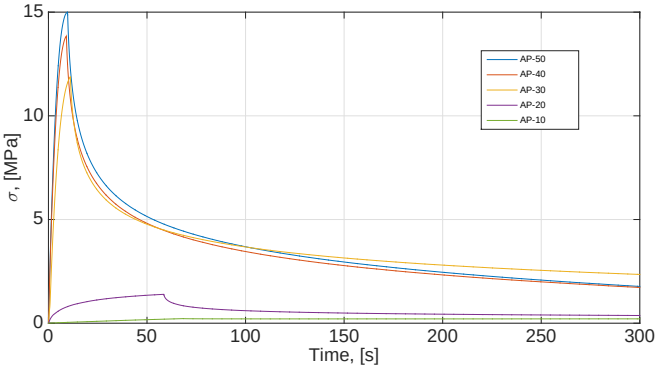

Fig. 13 Relaxation for as-prepared specimens over time.

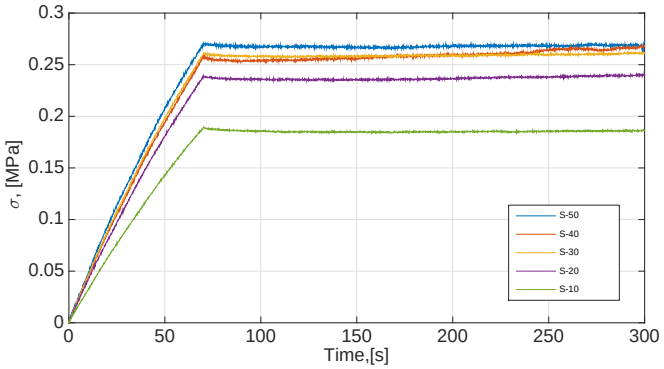

Fig. 14 Relaxation for fully swollen specimens over time.

4.4 Cyclic loading of as-prepared and fully swollen hydrogels

Relation between the degree of swelling and the plastic deformation was evaluated through cyclic loading using a controlled strain program. During the first cyclic loading, as-prepared sample of HEMA-10 displayed a residual strain of ϵ_{res} = 2.9 % , whereas the same specimen in its fully swollen state exhibited a decrease in stress and a lower residual strain of ϵ_{res} = 1.6 % after the final cyclic loading as depicted in Fig. 15.

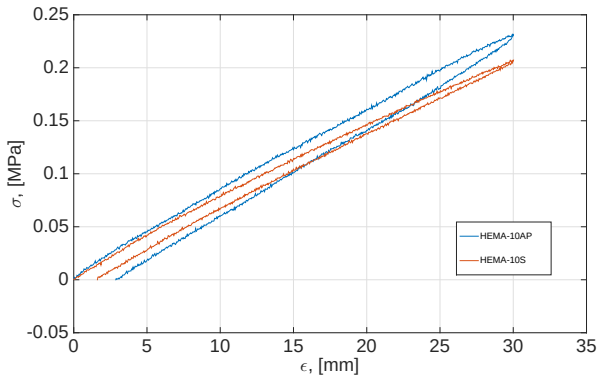

Fig. 15 Cyclic loading of HEMA-10 interrupted by swelling.

5. Discussion

During this study, hydrogels were manufactured via photo-initiated polymerization at various water:monomer mixture concentrations; i.e. water concentration is constant (Table I). Analysis of the effects of varying the monomer concentration upon swelling and mechanical properties is performed. Fitting of experimental data lead to the acquisition of material parameters used for further validation of the mathematical model using constitutive equations.

Comparison of sample series show a dependency of monomer concentration to the equilibrium degree of swelling. Specifically it is shown that a higher monomer concentration leads to a lower equilibrium and initial

degree of swelling. Since the fraction of monomer is increased for the same amount of water concentration, it is expected that the initial and equilibrium degree of swelling will be different due to the formation of a more dense material. By definition, a less porous hydrogel leads to lower amount of water molecules to diffuse into the network. The decrease in swelling observed for as-prepared HEMA-5 specimens is attributed to an extensively swollen state after polymerization (Q_0 = 1 g/g), which is above the maximum value of the average degree of swelling ($\bar{Q} \approx 0.85$ g/g) found in this study. Consequently, the elastic free energy of the cross-linked network is initially higher than that of the free energy of mixing from the polymer and solvent interaction. This leads to the expulsion of water molecules from the hydrogel network until an equilibrium between the elastic energy and energy of mixing is achieved.

Fig. 2 displays a difference in swelling kinetics between spherical and thin plate samples, at which the equilibrium degree of swelling for spheres is reached at a faster time. This is in good agreement with Li and Tanaka (1990) where it was shown that the swelling kinetics are affected by the shape of the specimens [26]. Furthermore, the decrease in $\bar{Q}$ amidst each series immersed in 1M of NaCl solution might be explained by the decrease in χ parameter. Since interactions between segments of chains and water molecules are accounted for through the Flory-Huggins parameter, it is believed that the reduction of χ may be due to the addition of salt into the water bath, thus diminishing the swelling response of HEMA hydrogels and subsequently the equilibrium degree of swelling.

Tensile tests reveal that the swelling degree alters the stress-strain response of hydrogels. Concentration of monomer strongly affects the mechanical response of HEMA gels in their as-prepared state, which as observed can produce different tensile behavior. Specifically, it is observed that a higher monomer concentration (and lower degree of swelling correspondingly) leads to an increase of stresses. Hydrogels during their fully swollen state exhibit differences in stress which are significantly lower in comparison to their as-prepared state. The small difference observed in tensile behavior of as-prepared samples HEMA-50 and 40 is believed to occur due to a high monomer concentration; i.e. 1:10 water:monomer mixture, which may lead into an incomplete reaction during polymerization. Thus causing a small amount of un-reacted monomer to be trapped in the network.

However, investigations for un-reacted monomer in the water bath through FTIR and UV spectroscopy did not reveal any presence of un-reacted species. Therefore the above assumption is deemed uncertain.

Hydrogels in their fully swollen state, except HEMA-10 and 5 indicate an equilibrium degree of swelling in-between 0.48 and 0.55 g/g resulting to a relatively similar elastic modulus. The elastic moduli tends to reduce insignificantly from HEMA-50 to 20 (from 0.39 MPa to 0.36 MPa) which corresponds to the small difference in the equilibrium degree of swelling. Experimental data from Fig. 9 are approximated through Eq. 19 in which the elastic modulus *G* is calculated for both as-prepared and fully swollen specimens, resulting to Fig. 10.

Relaxation tests on as-prepared specimens display a visco-elastic behavior as the stress reduces over time. However the visco-elastic effect is not observed for HEMA-10 and 5 due to the apparent constant stress during the first 4 minutes after relaxation is initiated. Fully swollen specimens after approximately 4 minutes of relaxation exhibit a slight increase in stress, which can be attributed to the formation of a rigid "skin" on the its surface or due to evaporation of water from its network.

Plastic deformation is evaluated by subjecting hydrogels in cyclic loading interrupted by swelling. Fig. 15 shows that swelling of the samples up to their equilibrium degree of swelling reduces the initial residual strain induced from the first loading cycle. The almost twofold decrease in residual strain is attributed to the self-recovery phenomenon which is in good agreement with Drozdov et.al. (2015) [13]. Hydrogels in their swollen state along with HEMA-10 and 5 are treated as an elastic medium, through which is further supported by the mechanical experiments performed (Fig. 13-15).

Through the governing equations developed, three material parameters are acquired, in which for a given composition swelling kinetics can be simulated. These include (i) the Flory-Huggins parameter χ, (ii) the dimensionless elastic modulus *g* and (iii) diffusivity D_0. Following the simulation, χ parameter was determined to range from HEMA-50 to HEMA-5 from 0.985 to 0.798 respectively. HEMA-10, manufactured in this study, illustrates a χ = 0.878 which deviates the least from the values found in previous studies and specifically, χ = 0.82 [27], χ = 0.841 [28] and χ = 0.853 [29]. Equivalent diffusivity parameters from HEMA-50 to HEMA-10 is ranging between D_0 = 5.87 10^{-6} and D_0 = $4.89 \cdot 10^{-6}$ cm^2/s, whereas for HEMA-5 is $6.75 \cdot 10^{-6}$. Diffusivity in a previous study was found to be D_0 = 4.4 $\cdot$ 10^{-6} cm^2/s determined through NMR spectroscopy. Hence, it is concluded that HEMA-10 discs and both

of HEMA-10 spheres χ = 0.853 and χ = 0.864 along with D_0 = 4.91$\cdot$ 10^{-6} and D_0 = 4.7$\cdot$ 10^{-6} cm^2/s are in very good agreement with previous studies. This implies that a composition of water:monomer mixture (1:2) can be considered the most appealing regarding HEMA gels swelling and mechanical behavior.

6. Conclusion

2-hydroxyethyl(methacrylate) based hydrogels were manufactured at various water to monomer concentrations via photo-initiated polymerization, in solution. Swelling and mechanical properties were investigated and compared for each composition. Initial and equilibrium degree of swelling were found to increase while the monomer concentration decreases, explained by the formation of a more porous network. Swelling of hydrogels immersed in salt solution indicated a lower equilibrium degree of swelling revealing an inverse response to the overshooting effect.

Uniaxial tensile tests illustrated a dependance of mechanical properties upon swelling and specifically stresses are reduced as the monomer concentration is lowered. A region has been found at which hydrogels lose their stress-relaxation determined to be approximately 40-45 % of swelling. Hypothesis of self-recovery induced by swelling is not rejected since a decrease in residual plastic strain was observed through uniaxial cyclic loading.

A mathematical model developed for transport of solvent using constitutive equations with finite deformations for swelling of hydrogels is utilized. Material parameters, such as dimensionless elastic modulus, Flory-Huggins solubility parameter and equivalent diffusivity were determined by fitting of experimental data to the model. Good agreement between experimental and simulation data has been found, which further supports the validity of the governing equations developed. HEMA-10 composition is believed to be the most preferable amongst all others, since it illustrates a satisfying set of material parameters which are in good agreement with previous studies.

References

[1] O.Wichterle and D.Lim, "Hydrophilic gels for biological use," *Nature*, vol. 185, no. 4706, pp. 117–118, 1960.

[2] E. M. Ahmed, "Hydrogel: preparation, characterization and applications, a review," *Journal of Advanced Research*, vol. 6, no. 2, pp. 105–121, 2015.

[3] T. R. Hoare and D. S. Kohane, "Hydrogels in drug delivery, progress and challenges," *Polymer*, vol. 49, no. 8, pp. 1993–2007, 2008.

[4] S. Anisha, S. P. Kumar, G. V. Kumar, and G. Garima, "Hydrogels a review," *International Journal of Pharmaceutical Sciences Review and Research*, vol. 4, no. 16, 2010.

[5] M.W.Tibbitt and K.S.Anseth, "Hydrogels as extracellular matrix mimics for 3d cell culture," *Biotechnology and Bioengineering*, vol. 103, no. 4, pp. 655–663, 2009.

[6] G. Huang, L. Wang, S. Wang, Y. Han, J. Wu, Q. Zhang, F. Xu, and T. J. Lu, "Engineering three-dimensional cell mechanical microenvironment with hydrogels," *Biofabrication*, vol. 4, no. 4, p. 042001, 2012.

[7] E. Calo and V. V. Khutoryanskiy, "Biomedical applications of hydrogels a review of patents and commercial products," *European Polymer Journal*, vol. 65, pp. 252–267, 2015.

[8] L. Zhang, K. Li, W. Xiao, L. Zheng, Y. Xiao, H. Fan, and X. Zhang, "Preparation of collagen-chondroitin sulfate-hyaluronic acid hybrid hydrogel scaffolds and cell compatibility in vitro," *Carbohydrate Polymers*, vol. 84, no. 1, pp. 118–125, 2011.

[9] X. Lou and C. van Coppenhagen, "Mechanical characteristics of poly(2-hydroxyethyl methacrylate) hydrogels crosslinked with various dysfunctional compounds," *Polymer International*, vol. 50, pp. 319–325, 2001.

[10] J. Lee and D. Buchnall, "Swelling behavior and network structure of hydrogels synthesized using controlled uv-initiated free radical polymerization," *J. Polym. Sci. B:Polymer Physics*, vol. 46, pp. 1450–1462, 2008.

[11] J. Weaver, I. Bannister, K. Robinson, X. Bories-Azeau, S. Armes, M. Smallridge, and P. McKenna, "Stimulus-responsive water-soluble polymers based on 2-hydroxyethyl methacrylate," *Macromolecules*, vol. 37, pp. 2395–2403, 2004.

[12] G. Mathur, L. Kandpal, and A. Sen, *Recent advances in polymers and composites*. Allied Publishers ltd., 2000.

[13] A. Drozdov, C. Sanporean, and J. Christiansen, "Mechanical response of hema gel under cyclic deformation: Viscoplasticity and swelling-induced recovery," *International Journal of Solids and*

Structures, vol. 52, pp. 220–234, 2015.

[14] J.-Y. Sun, X. Zhao, W. R. Illeperuma, O. Chaudhuri, K. H. Oh, D. J. Mooney, J. J. Vlassak, and Z. Suo, "Highly stretchable and tough hydrogels," *Nature*, vol. 489, no. 7414, pp. 133–136, 2012.

[15] K. S.Anseth, C. N.Bowman, and L. Brannon-Peppas, "Mechanical properties of hydrogels and their experimental determination," *Biomaterials*, vol. 17, no. 17, pp. 1647–1657, 1996.

[16] J. Kurnia, E. Birgersson, and A. Mujumdar, "A phenomenological model for hydrogel with rigid skin formation," *Int. J. Appl. Mechanics*, vol. 04, no. 01, p. 1250007, 2012.

[17] W.D.Callister and D.G.Rethwisch, *Materials science and engineering, an introduction*. Wiley, 9 ed., 2013.

[18] F. Jiang, T. Huang, C. He, H. R.Brown, , and H. Wang, "Interactions affecting the mechanical properties of macromolecular microsphere composite hydrogels," *The Journal of Physical Chemistry B*, vol. 117, pp. 13679–13687, 2013.

[19] M. A. Haque, T. Kurokawa, G. Kamita, and J. P. Gong, "Lamellar bilayers as reversible sacrificial bonds to toughen hydrogel: hysteresis, self-recovery, fatigue resistance and crack blunting," *Macromolecules*, vol. 44, pp. 8916–8924, 2011.

[20] T. Nakajima, T. Kurokawa, S. Ahmed, W. li Wud, and J. P. Gong, "Characterization of internal fracture process of double network hydrogels under uniaxial elongation," *Soft Matter*, vol. 9, pp. 1955–1966, 2012.

[21] S. Rose, A. Dizeux, T. Narita, D. Hourdet, and A. Marcellan, "Time dependence of dissipative and recovery processes in nanohybrid hydrogels," *Macromolecules*, vol. 46, pp. 4095–4104, 2013.

[22] A. Drozdov, A. Papadimitriou, J. Liely, and C. Sanporean, "Kinetics of swelling of hdrogels." submitted, 2016.

[23] K.-T. Huang and C.-J. Huang, "Novel zwitterionic nanocomposite hydrogel as effective chronic wound healing dressings," *IFMBE Proceedings, 1st Global Conference on Biomedical Engineering and 9th Asian-Pacific Conference on Medical and Biological Engineering*, vol. 47, no. 1, pp. 35–38, 2014.

[24] C. Li, L. Xu, M. Zhai, J. Peng, and J. Li, "Overshooting effect of poly(dimethylaminoethyl methacrylate) hydrogels," *Journal of Applied Polymer Science*, vol. 120, no. 4, pp. 2027–2033, 2011.

[25] Y. Yin, X. Ji, H. Dong, Y. Ying, and H. Zheng, "Study of the swelling dynamics with overshooting effect of hydrogels based on sodium alginate-g-acrylic acid," *Carbohydrate Polymers*, vol. 71, no. 4, pp. 682 – 689, 2008.

[26] L. Yong and T. Toyoichi, "Kinetics of swelling and shrinking of gels," *The Journal of Chemical Physics*, vol. 92, no. 2, pp. 1365–1371, 1990.

[27] F. Fornasiero, F. Krull, C. J. Radke, and J. M. Prausnitz, "Diffusivity of water through a hema-based soft contact lens," *Fluid Phase Equilibria*, vol. 228-229, pp. 269–273, 2005.

[28] A. Chauhan and C. J. Radke, "Permeability and diffusivity for water transport through hydrogel membranes," *Journal of Membrane Science*, vol. 2, no. 214, pp. 199–209, 2003.

[29] M.Ilavsky, K.Dusek, J.Vacik, and J.Kopeek, "Deformational swelling and potentiometric behavior of ionized gels of 2-hydroxyethyl methacrylate-methacrylic acid copolymers," *Journal of Applied Polymer Science*, vol. 23, no. 7, pp. 2073–2082, 1979.

Part I
Experimental Reports

Appendix A
Swelling in deionised water

A.1 Purpose

This experiment was performed to analyze the swelling properties of pHEMA gels in de-ionised water at different water:monomer concentrations. It's purpose is to determine how the degree of swelling is affected by the concentration of HEMA.

A.2 Sources of error

The samples are picked from water using polymer tongs in which high pressure on the sample should be avoided. In case of too high pressure applied the water might be pushed out of the hydrogel network. The weight measurements were performed on a digital scale with a precision of $\pm$ 1 mg.

A.3 Uncertainties

The conductivity of the de-water may have been altered when comes into contact with air, thus reducing the pH of the water. However this uncertainty is reduced by the renewal of water every 24 hours. Although each sample is wiped with paper in order to remove any excess of water on the surface, water may remain on the surface after wiping. The skin that was observed after polymerization of samples, was removed using a water:ethanol mixture and some may remain on the surface, affecting the swelling process.

A.4 Observations

UV polymerization was performed on one side of the samples, and it was observed that their surface appeared slightly different. The sample's surface that was in contact with the silicon mold resulted in the formation of a white skin.

A.5 Analysis and results

A.5.1 Swelling in water

Fig. A.1-A.7 display the swelling data obtained for each hydrogel specimen.

A.5.2 Swelling in 1M NaCl

Fig. A.8-A.12 displayed the data obtained for each specimens while swelling in 1M NaCl.

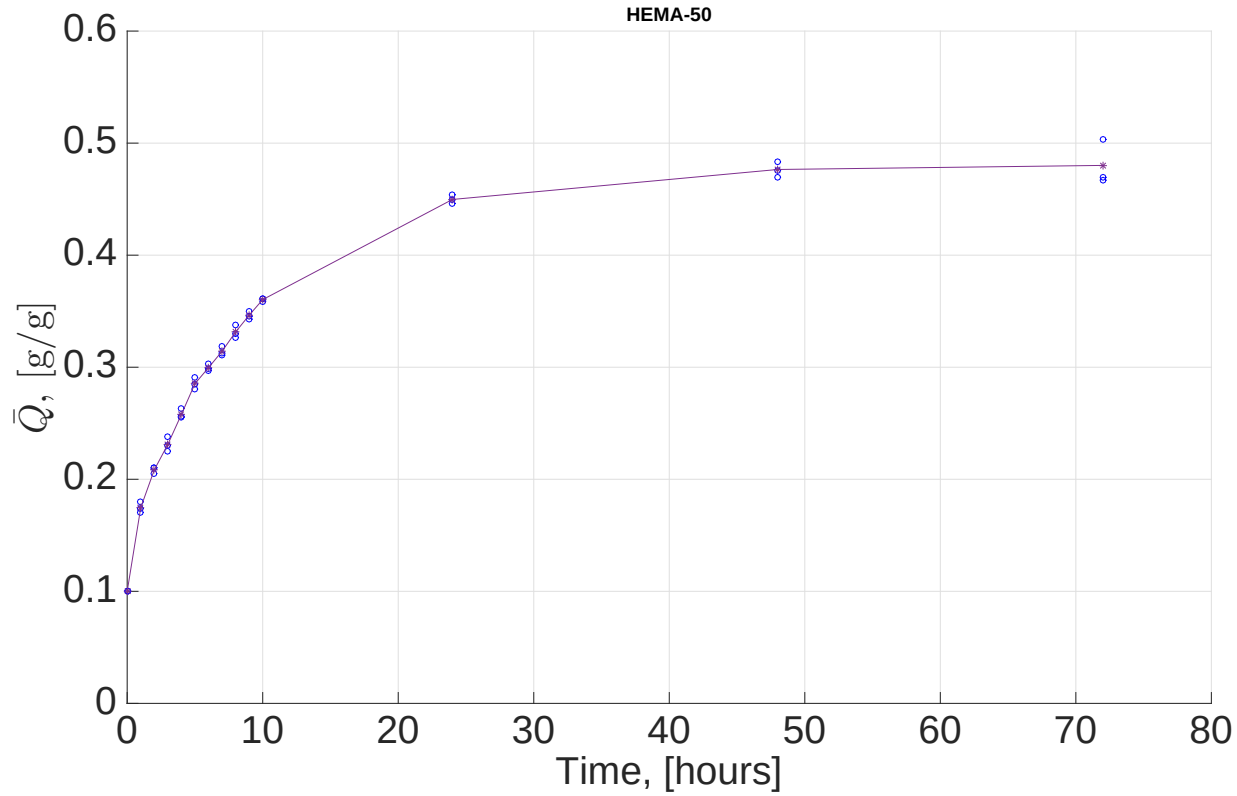

Fig. A.1 Average degree of swelling $\bar{Q}$ versus time t. Solid line: calculated mean, Circles: experimental data.

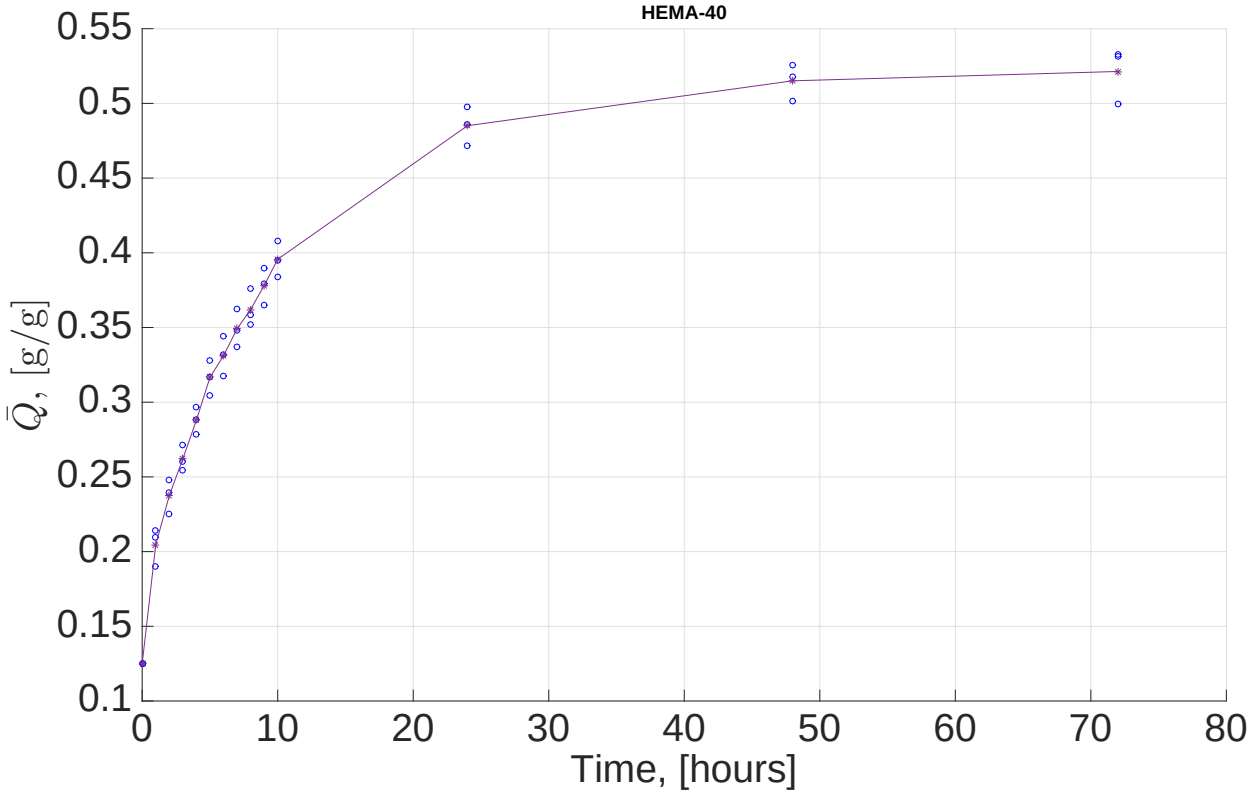

Fig. A.2 Average degree of swelling $\bar{Q}$ versus time t. Solid line: calculated mean, Circles: experimental data.

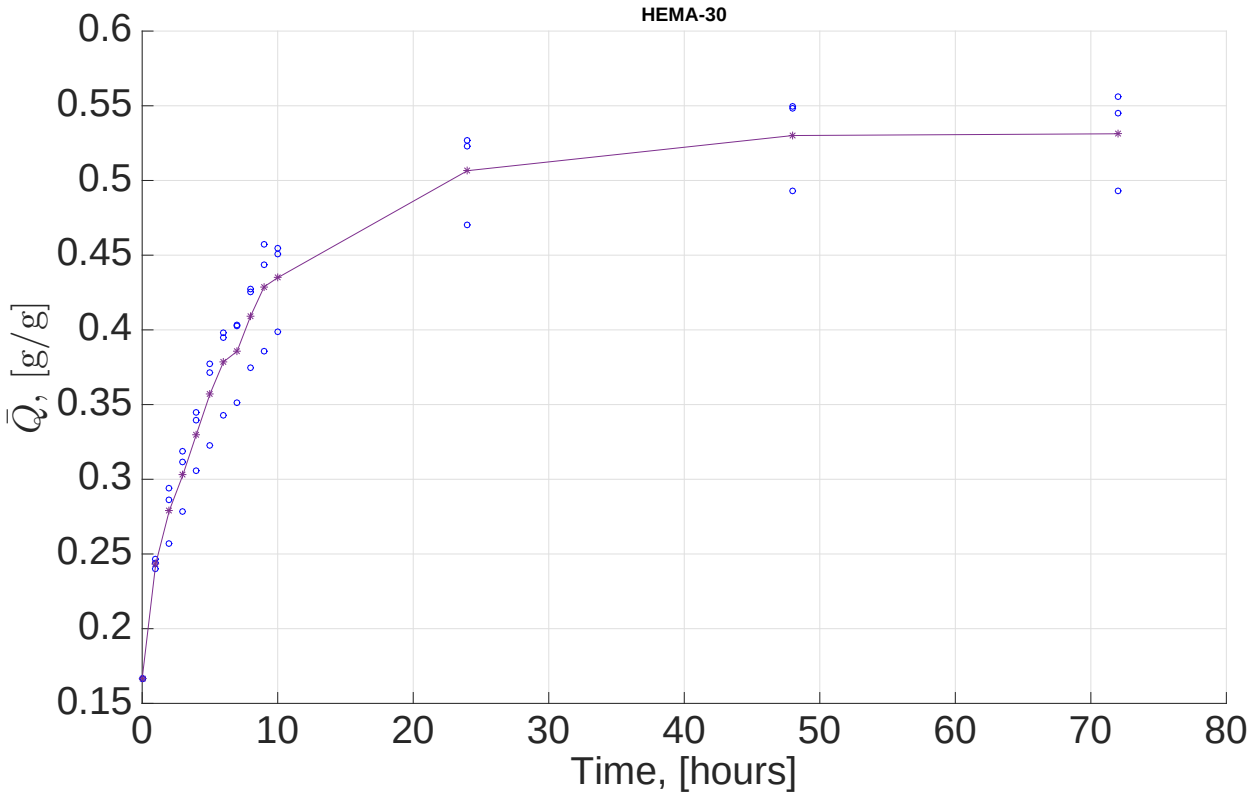

Fig. A.3 Average degree of swelling $\bar{Q}$ versus time t. Solid line: calculated mean, Circles: experimental data.

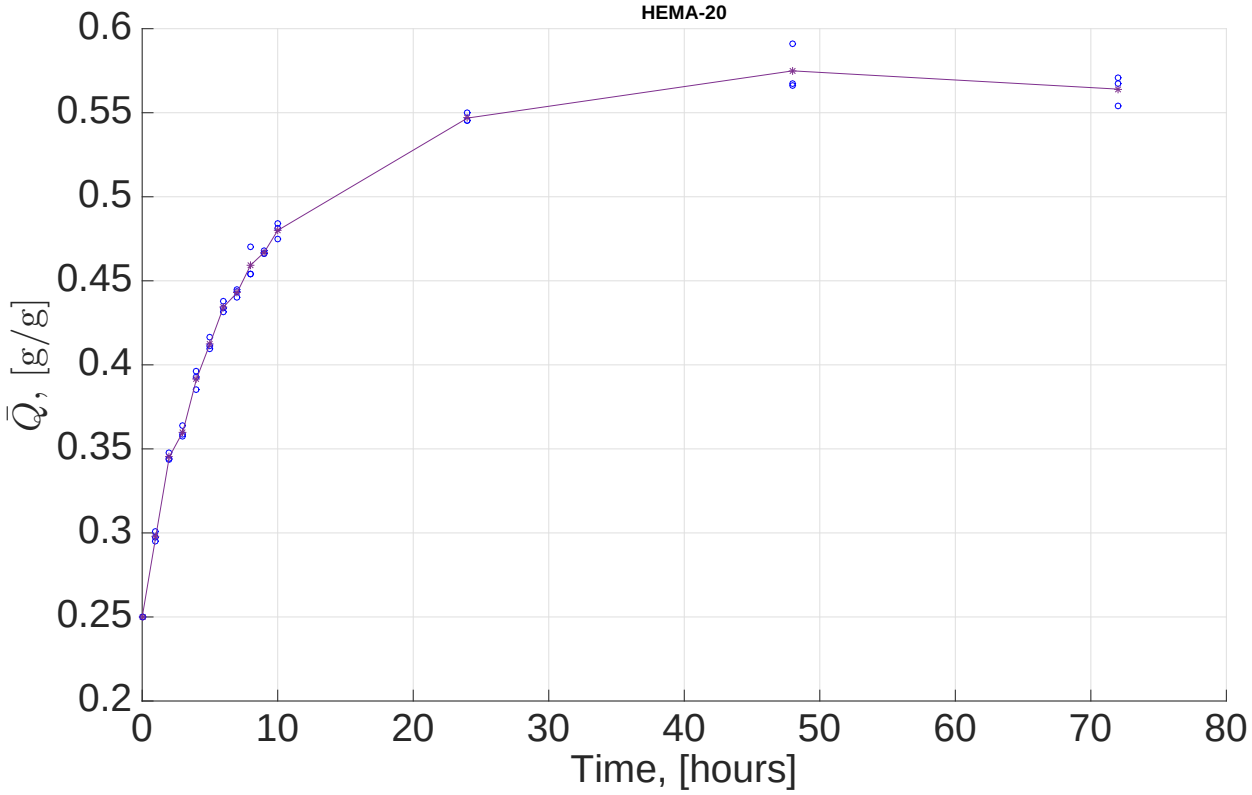

Fig. A.4 Average degree of swelling $\bar{Q}$ versus time t. Solid line: calculated mean, Circles: experimental data.

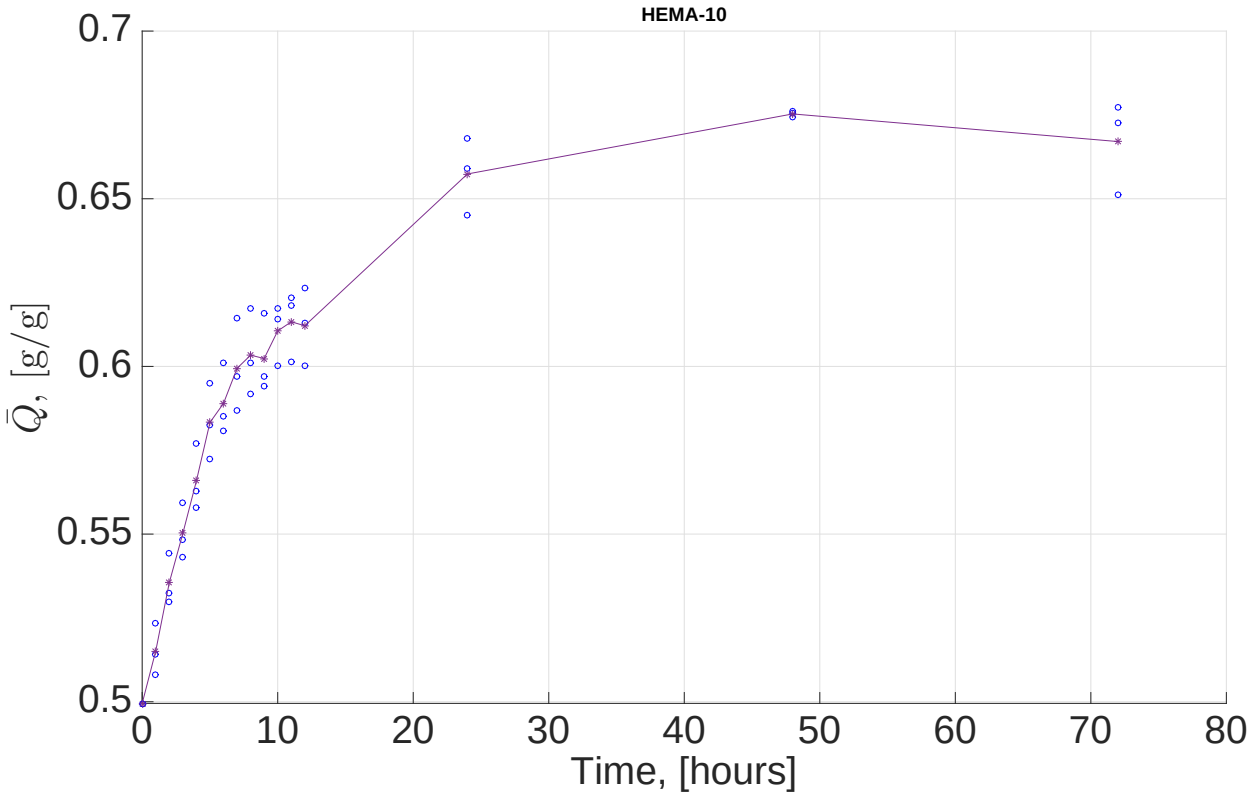

Fig. A.5 Average degree of swelling $\bar{Q}$ versus time t. Solid line: calculated mean, Circles: experimental data.

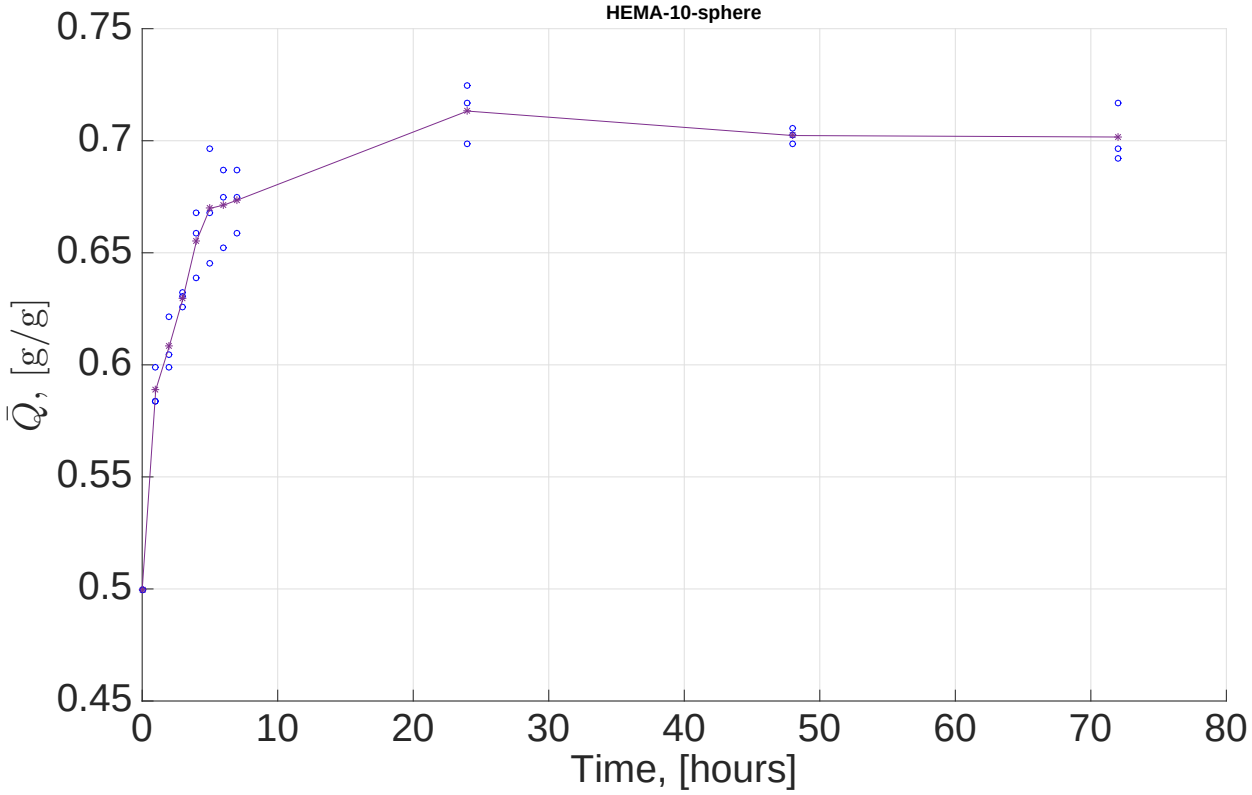

Fig. A.6 Average degree of swelling $\bar{Q}$ versus time t. Solid line: calculated mean, Circles: experimental data.

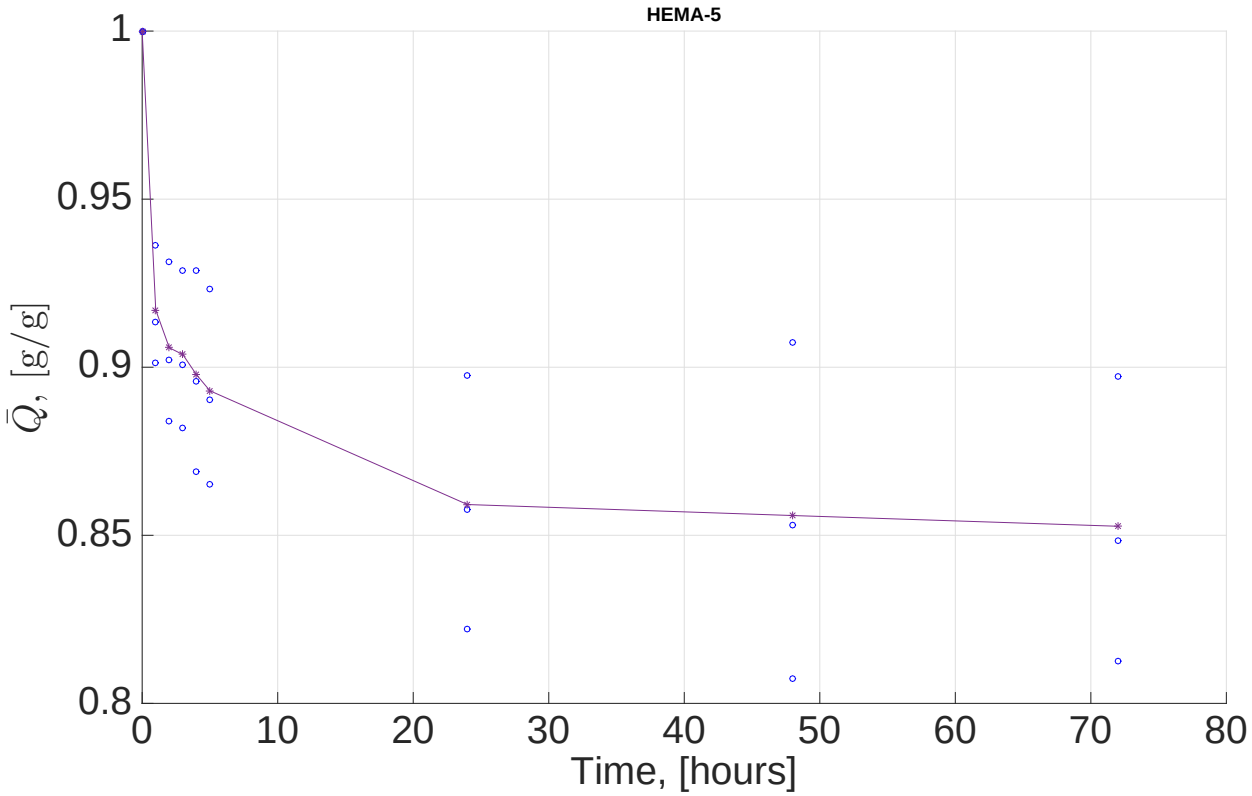

Fig. A.7 Average degree of swelling $\bar{Q}$ versus time t. Solid line: calculated mean, Circles: experimental data.

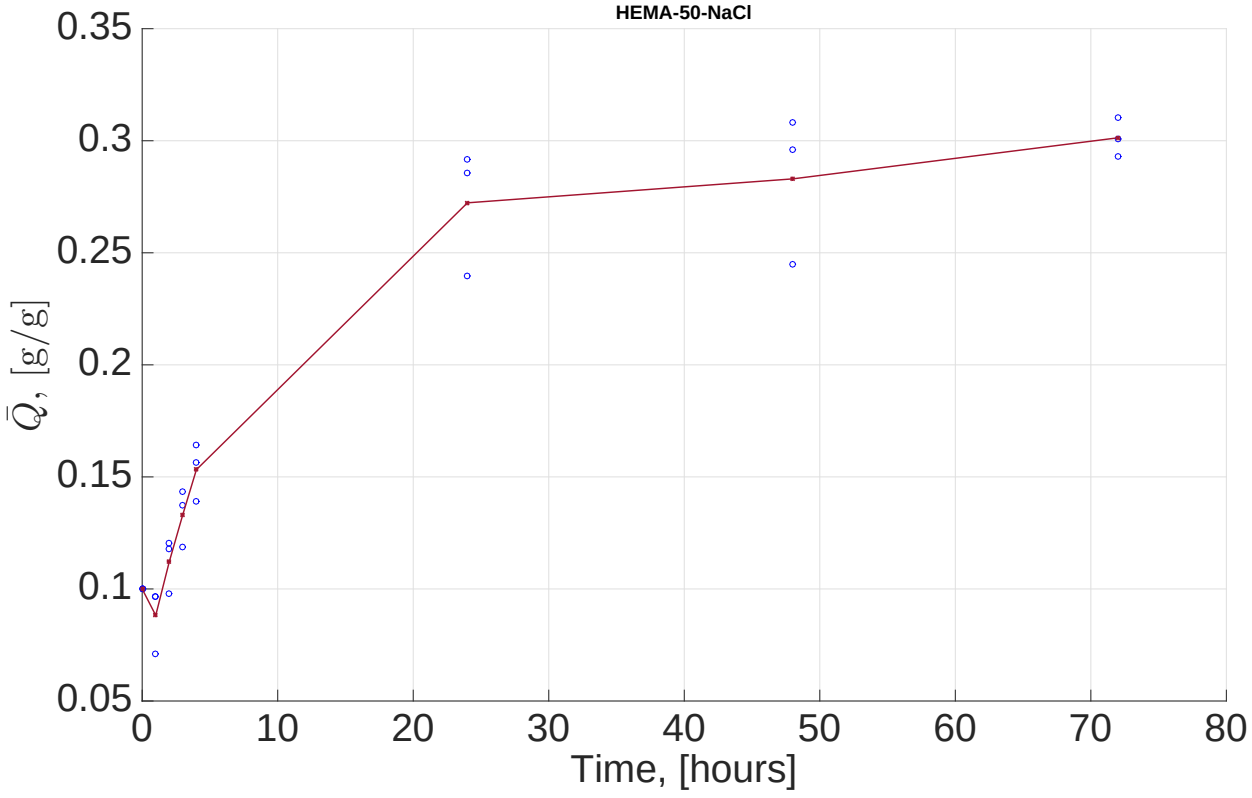

Fig. A.8 Average degree of swelling $\bar{Q}$ versus time t. Solid line: calculated mean, Circles: experimental data.

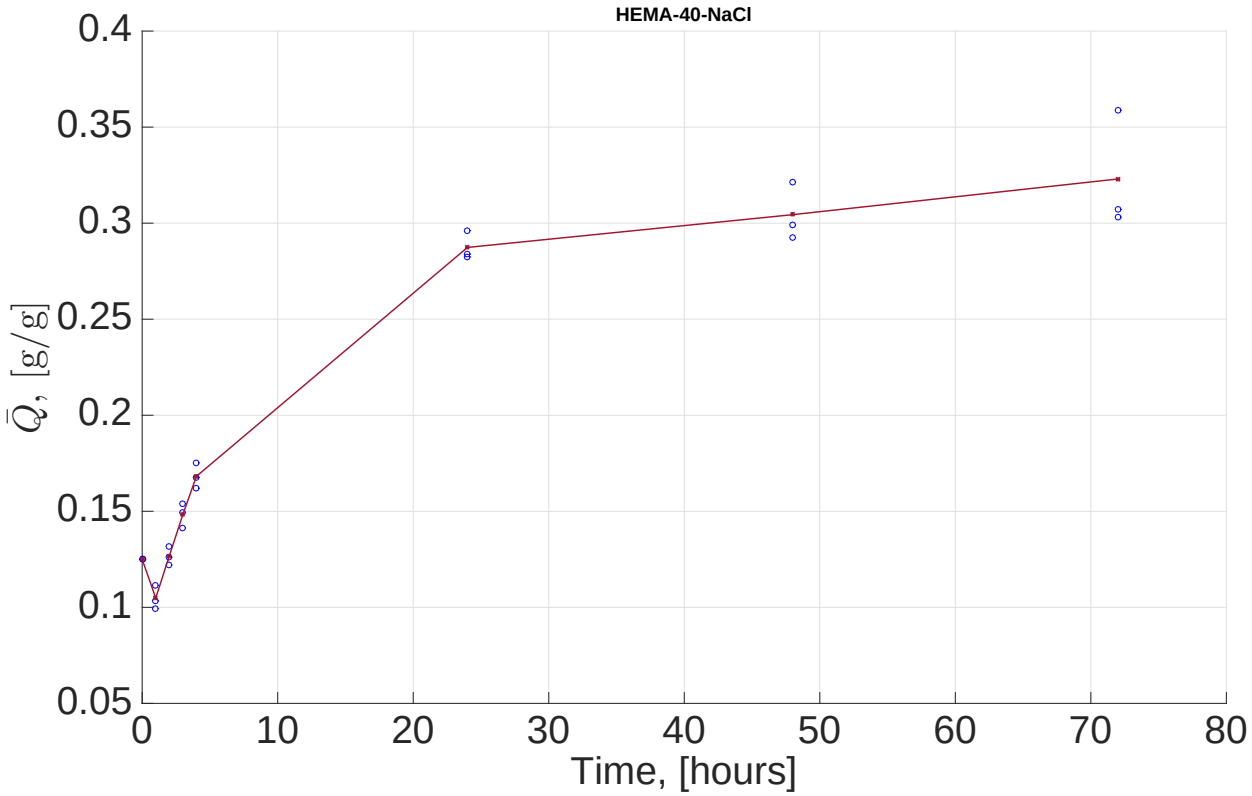

Fig. A.9 Average degree of swelling $\bar{Q}$ versus time t. Solid line: calculated mean, Circles: experimental data.

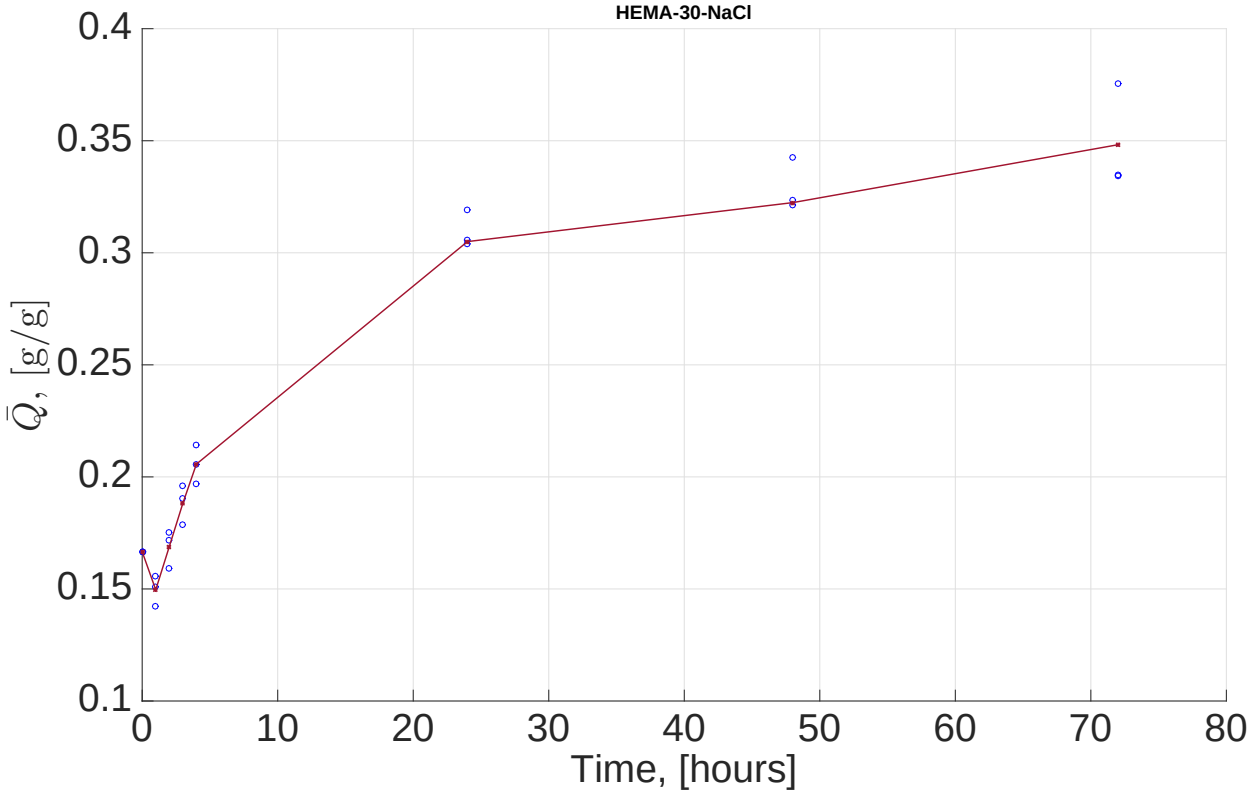

Fig. A.10 Average degree of swelling $\bar{Q}$ versus time t. Solid line: calculated mean, Circles: experimental data.

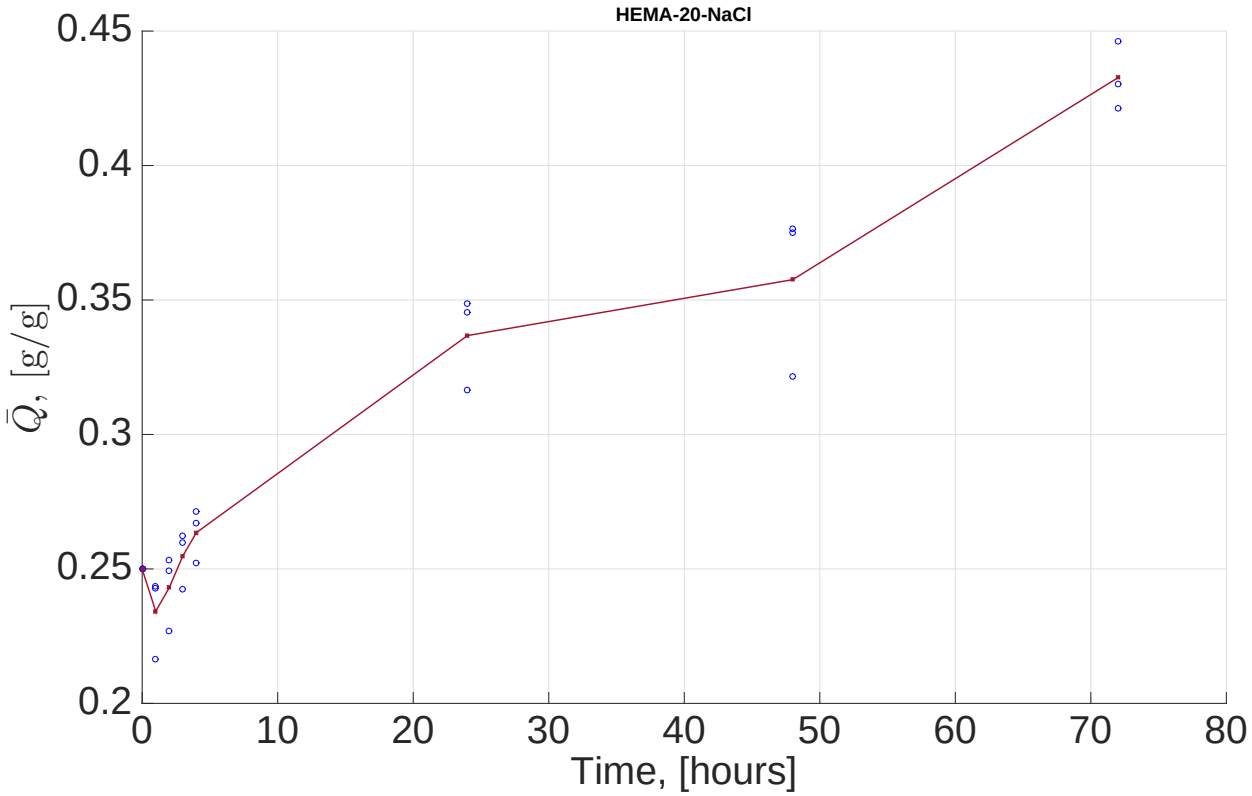

Fig. A.11 Average degree of swelling $\bar{Q}$ versus time t. Solid line: calculated mean, Circles: experimental data.

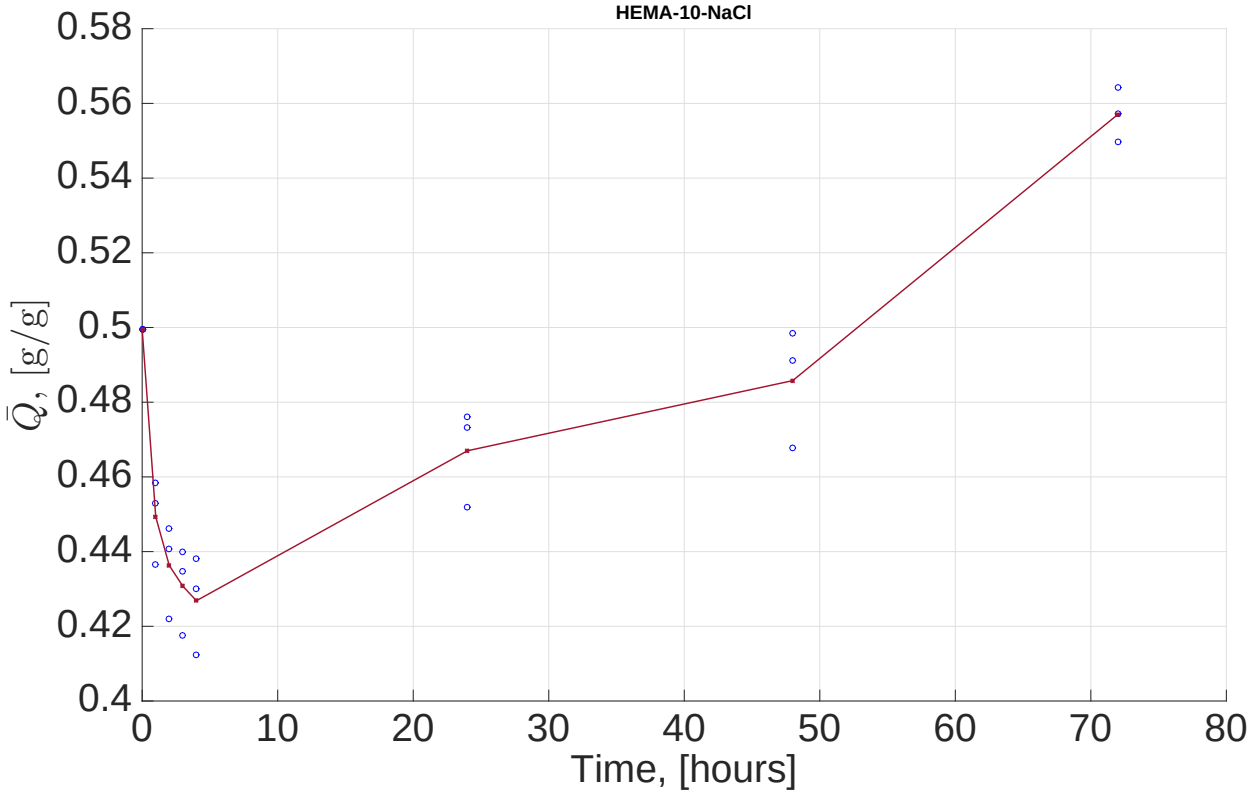

Fig. A.12 Average degree of swelling $\bar{Q}$ versus time t. Solid line: calculated mean, Circles: experimental data.

Appendix B
Uniaxial tension on pHEMA

B.1 Purpose

Uniaxial tests were performed to determine the mechanical properties of pHEMA hydrogels.

B.2 Sources of errors

The load cell used for the measurement had a maximum load of 2 kN. However, the load applied on the sample was in the order of 1-2 % of the maximum load thus creating noise during experimentation.

B.3 Uncertainties

When secured, the manual force applied by clamping samples may differ between each specimen. The cross sectional dimensions were defined from the mean of 3 different measurements. A digital caliper was used to measure both width and thickness at three different positions of the sample. Additionally, dimensional measurements of the fully swollen specimens may vary due to their rubber-like state; i.e. dimensions may appear smaller if too much force is applied from the caliper to the sample.

B.4 Observations

Some specimens were observed to break on the head of the specimens, which may discredit the strain at break measurements. A rigid skin was observed on the hydrogels surface, when samples are kept out of water more than 10 minutes during uniaxial test.

B.5 Analysis and results

B.5.1 Error bars for tensile test on as-prepared samples

Fig. B.13-B.18 display the statistical analysis done on as-prepared specimens using error bars.

B.5.2 Raw data of fully swollen specimens

Fig. B.19 and B.20 display the data obtained for 3 repetitions on each specimens.

B.5.3 Relaxation variance on swollen specimens.

Fig. B.23 and B.24 display the relaxation tests on 2 swollen specimens for each composition.

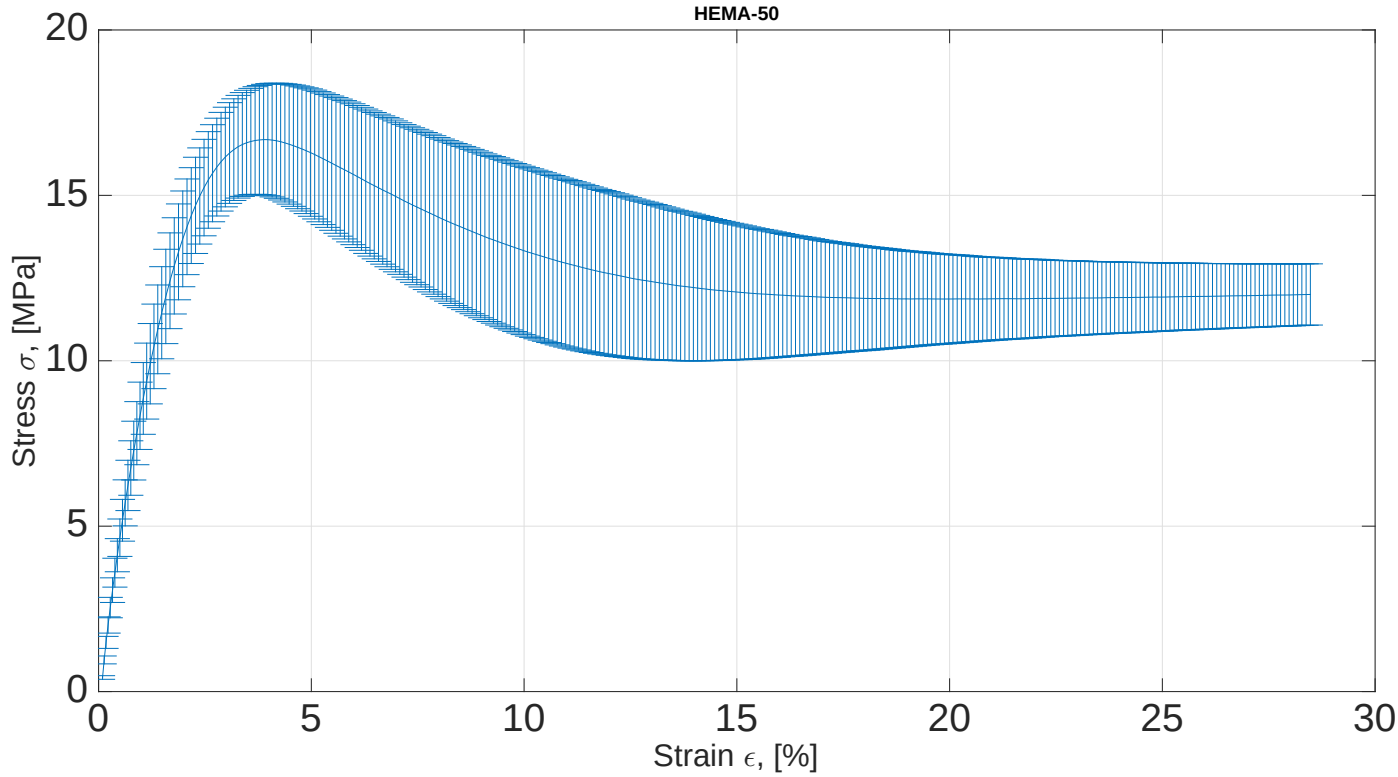

Fig. B.13 Stress σ versus strain ϵ along with error bars on as-prepared HEMA-50. Standard deviation of 2.55.

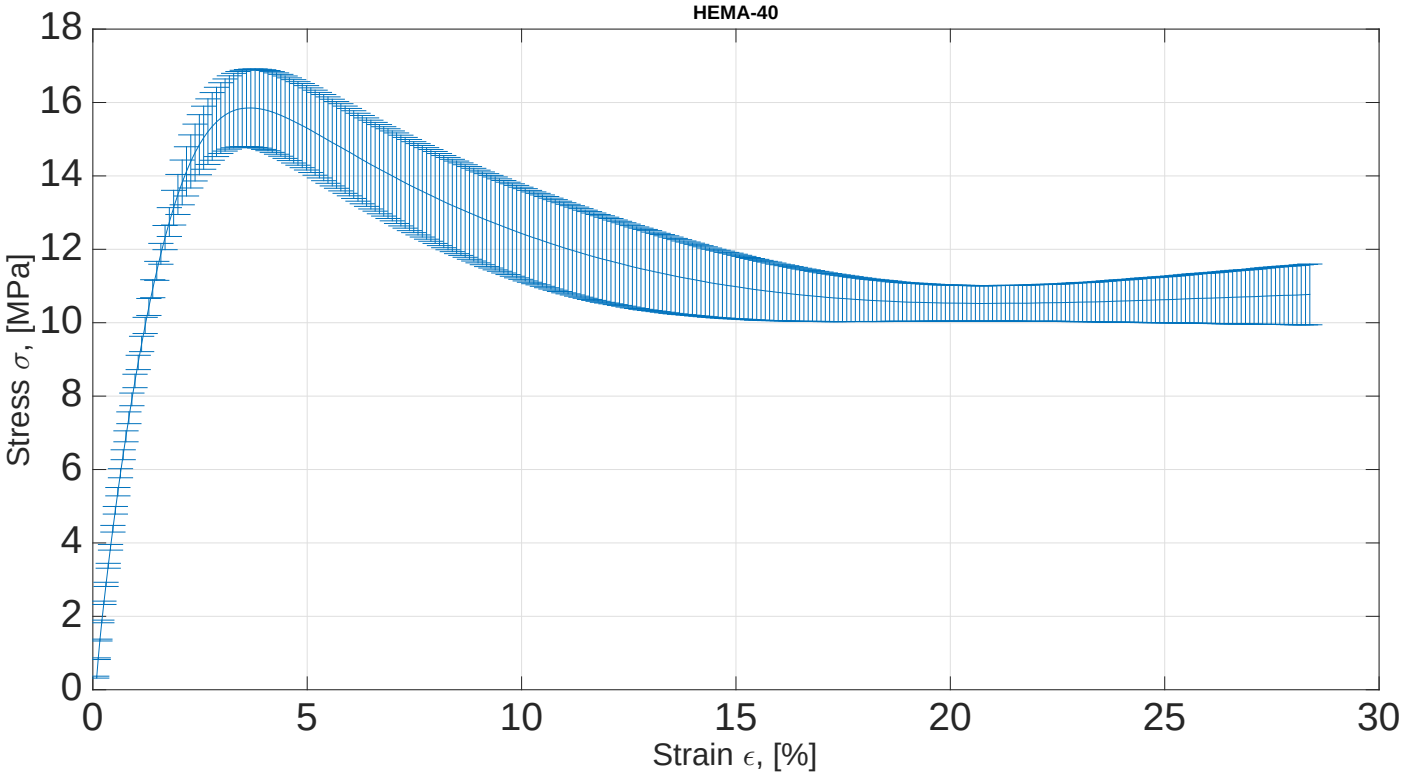

Fig. B.14 Stress σ versus strain ϵ along with error bars on as-prepared HEMA-40. Standard deviation of 1.78.

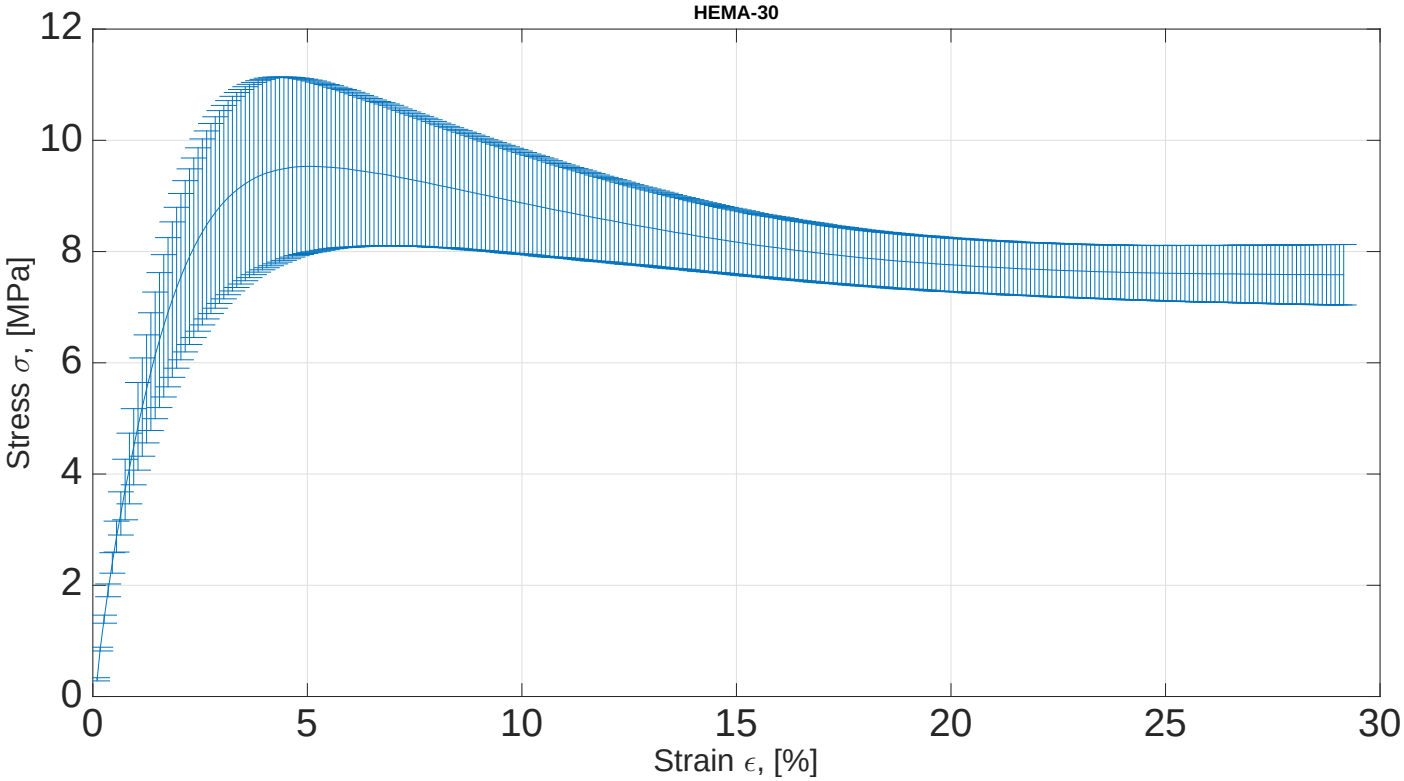

Fig. B.15 Stress σ versus strain ϵ along with error bars on as-prepared HEMA-30. Standard deviation of 1.75.

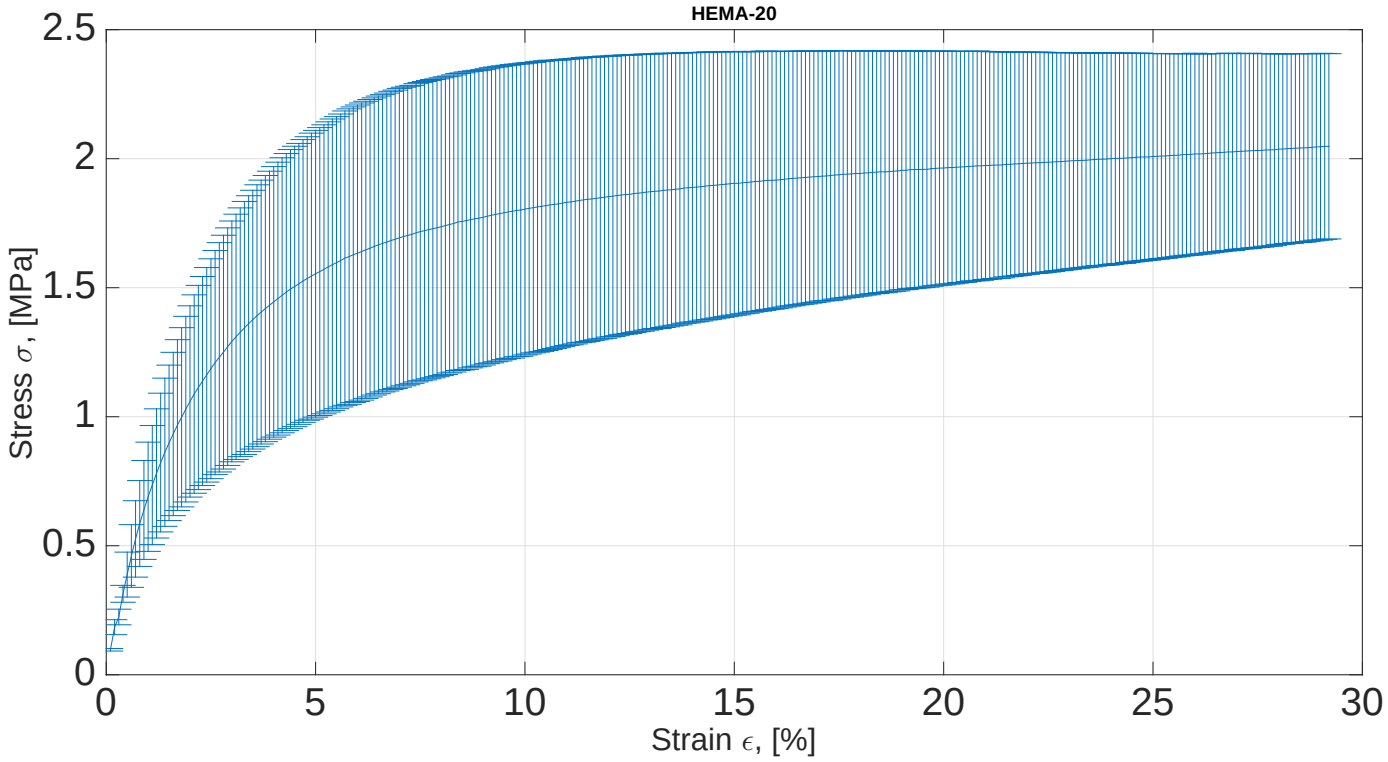

Fig. B.16 Stress σ versus strain ϵ along with error bars on as-prepared HEMA-20. Standard deviation of 0.58.

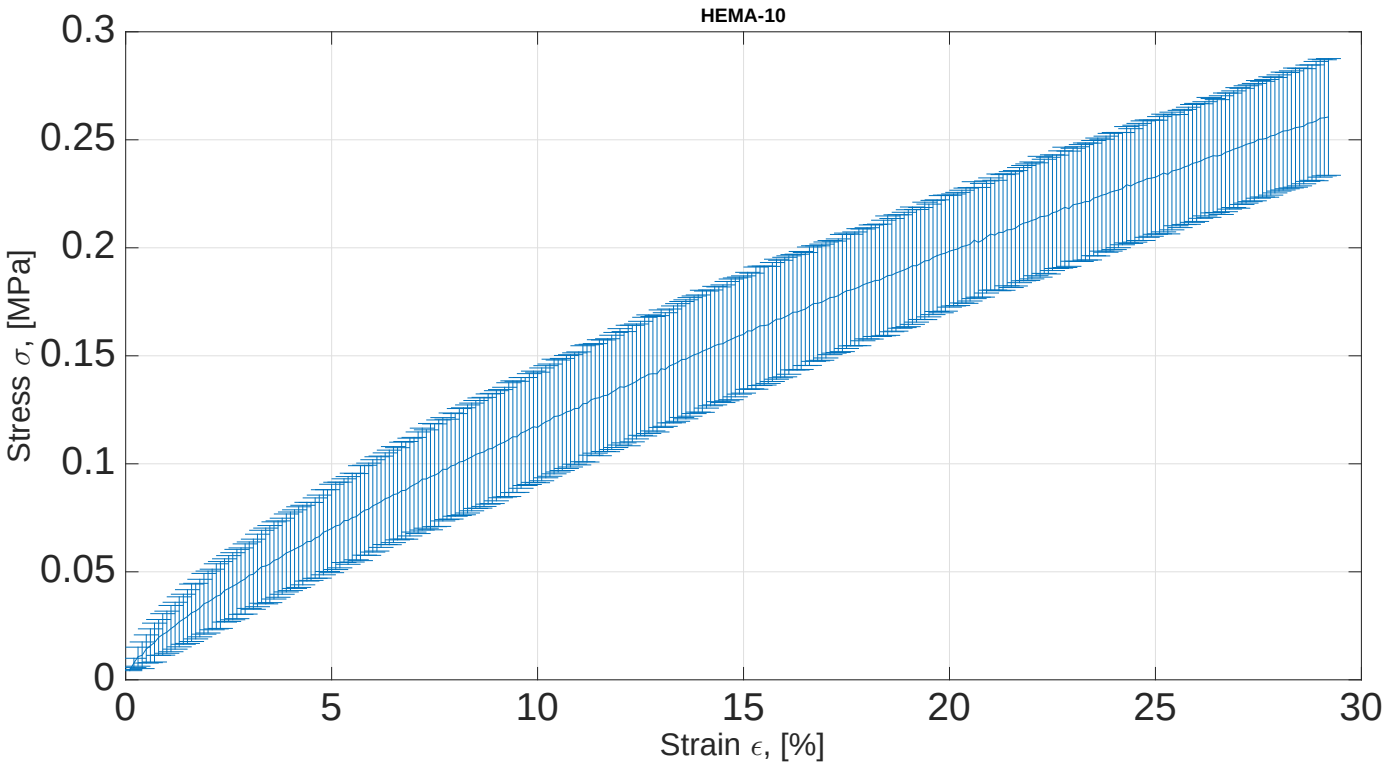

Fig. B.17 Stress σ versus strain ϵ along with error bars on as-prepared HEMA-10. Standard deviation of 0.03.

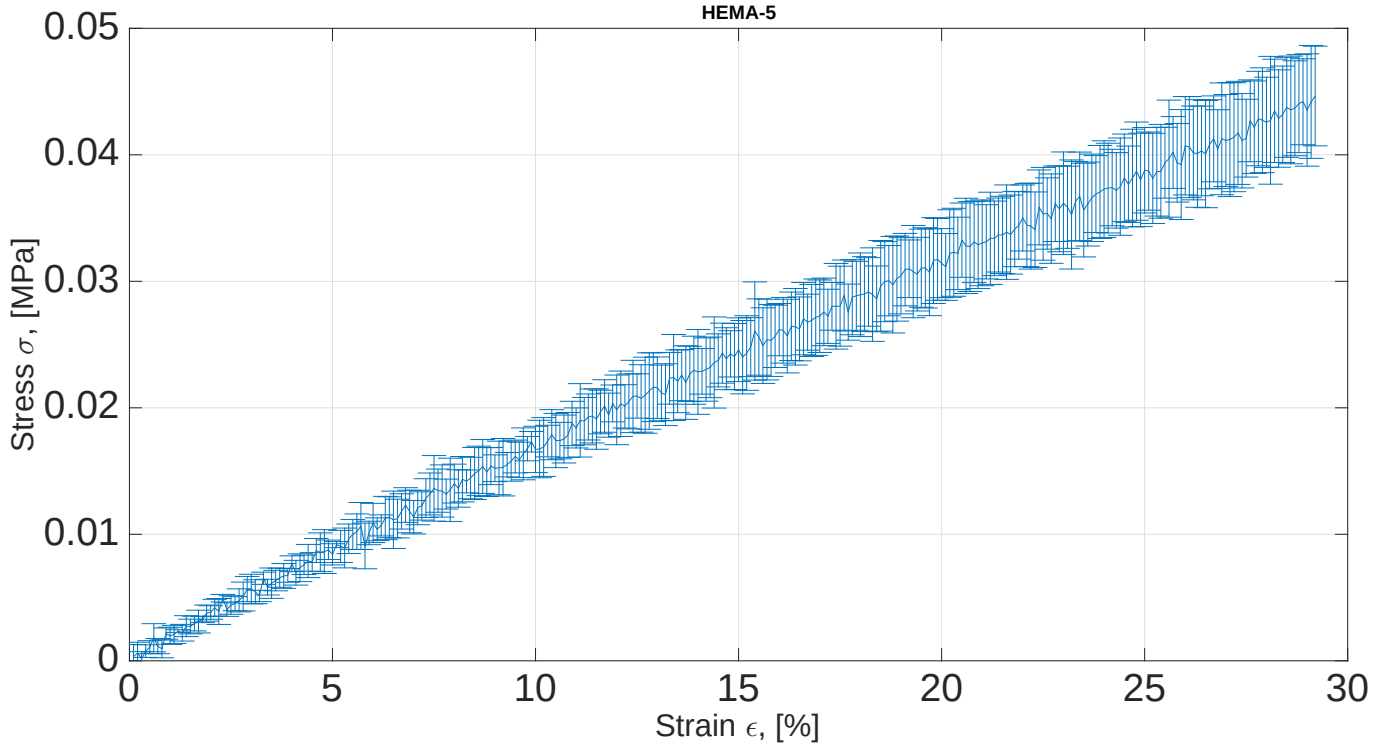

Fig. B.18 Stress σ versus strain ϵ along with error bars on as-prepared HEMA-5. Standard deviation of 0.01.

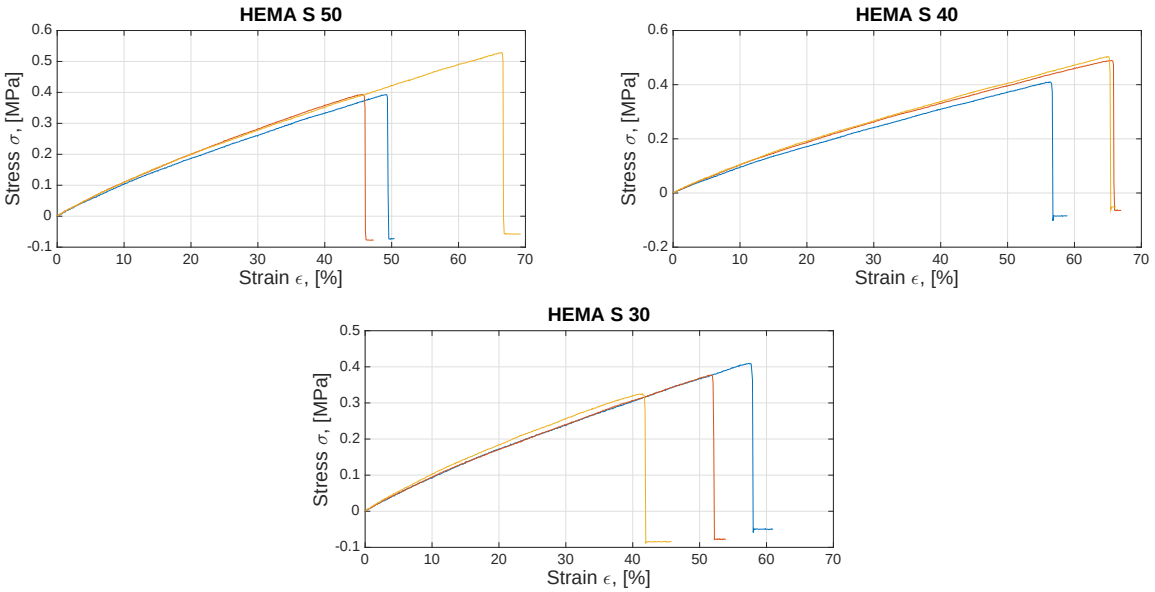

Fig. B.19 Stress σ versus strain ϵ on fully swollen specimens.

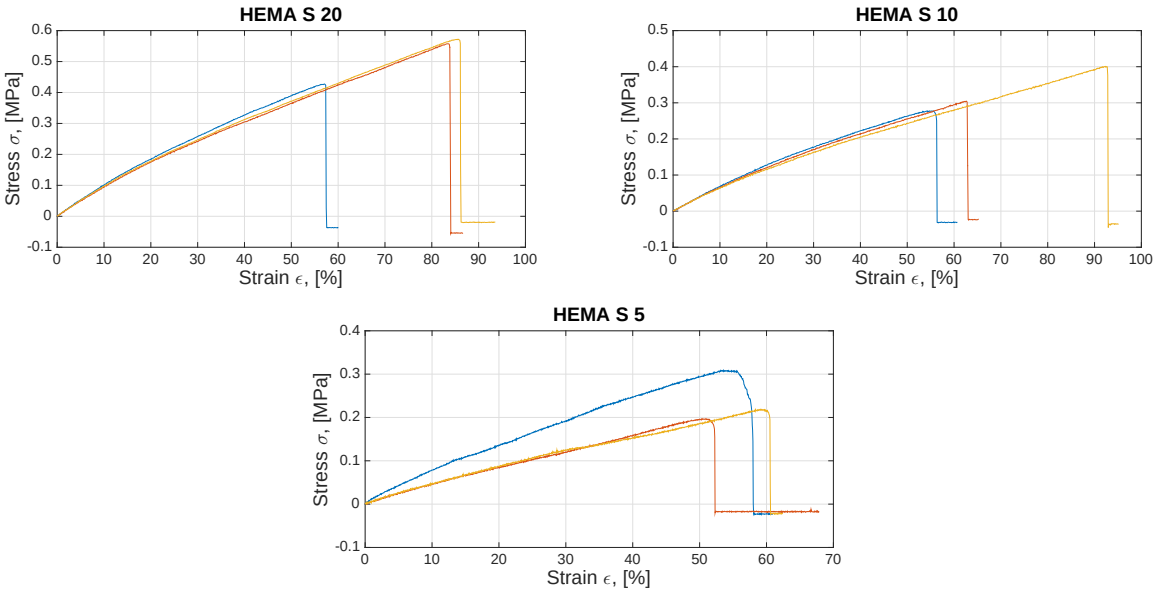

Fig. B.20 Stress σ versus strain ϵ on fully swollen specimens.

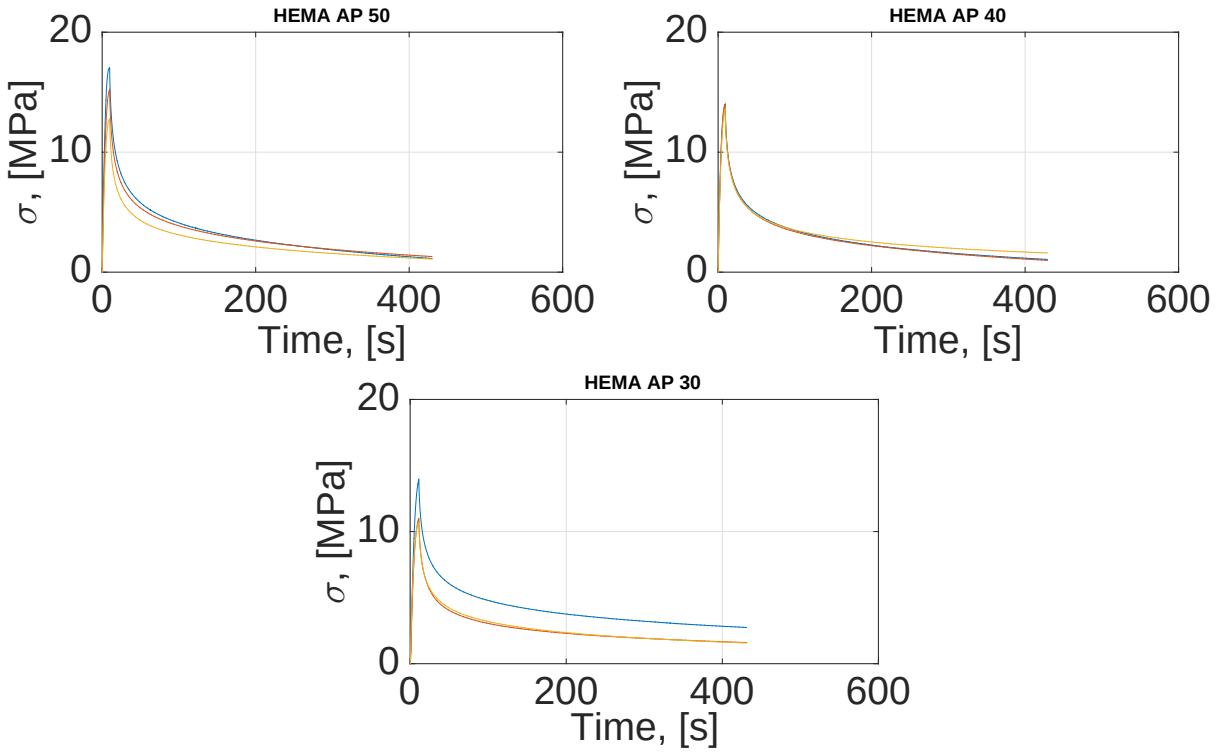

Fig. B.21 Stress σ versus time on as-prepared specimens.

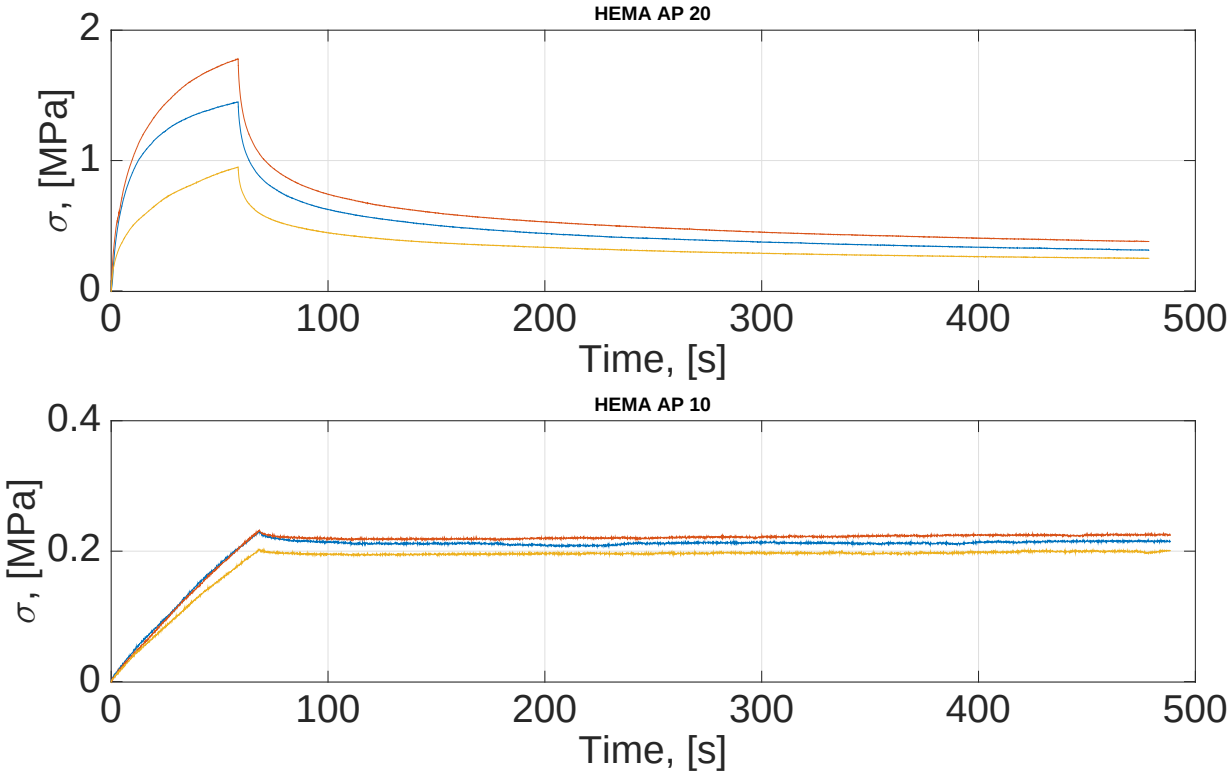

Fig. B.22 Stress σ versus time on as-prepared specimens.

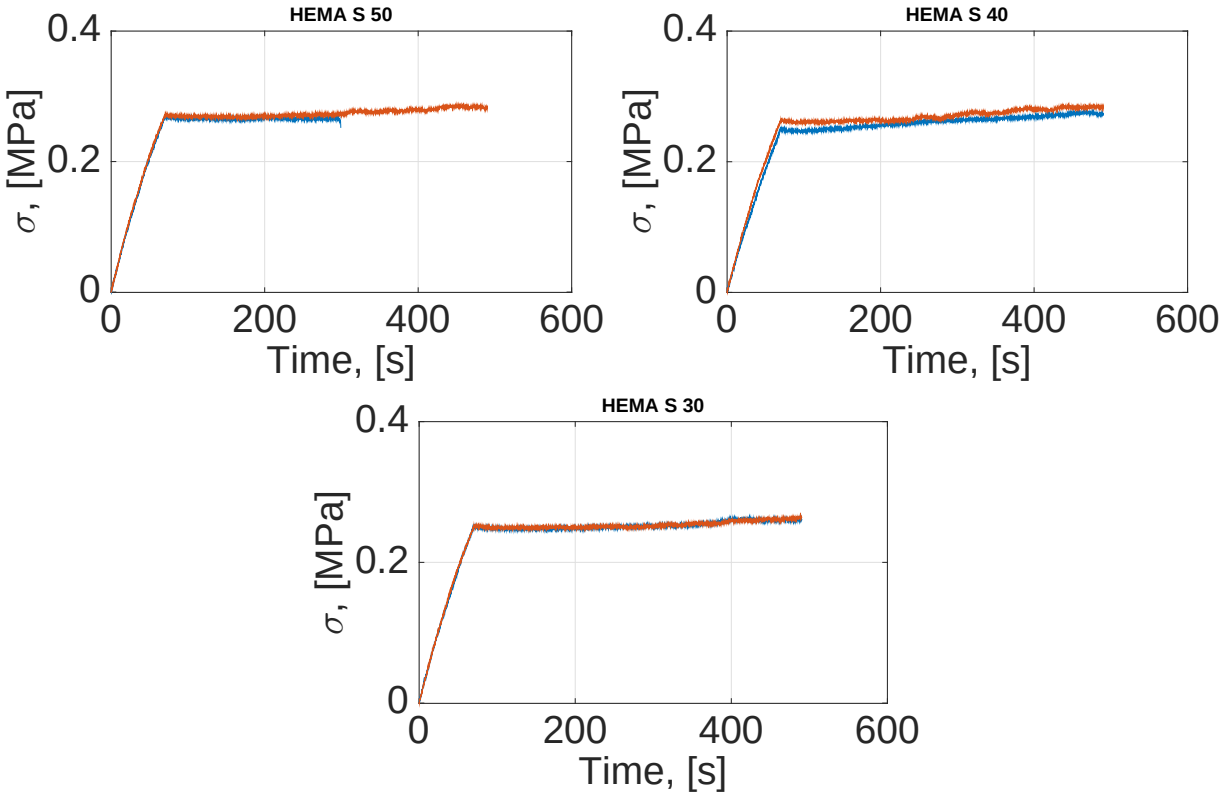

Fig. B.23 Stress σ versus time on swollen specimens.

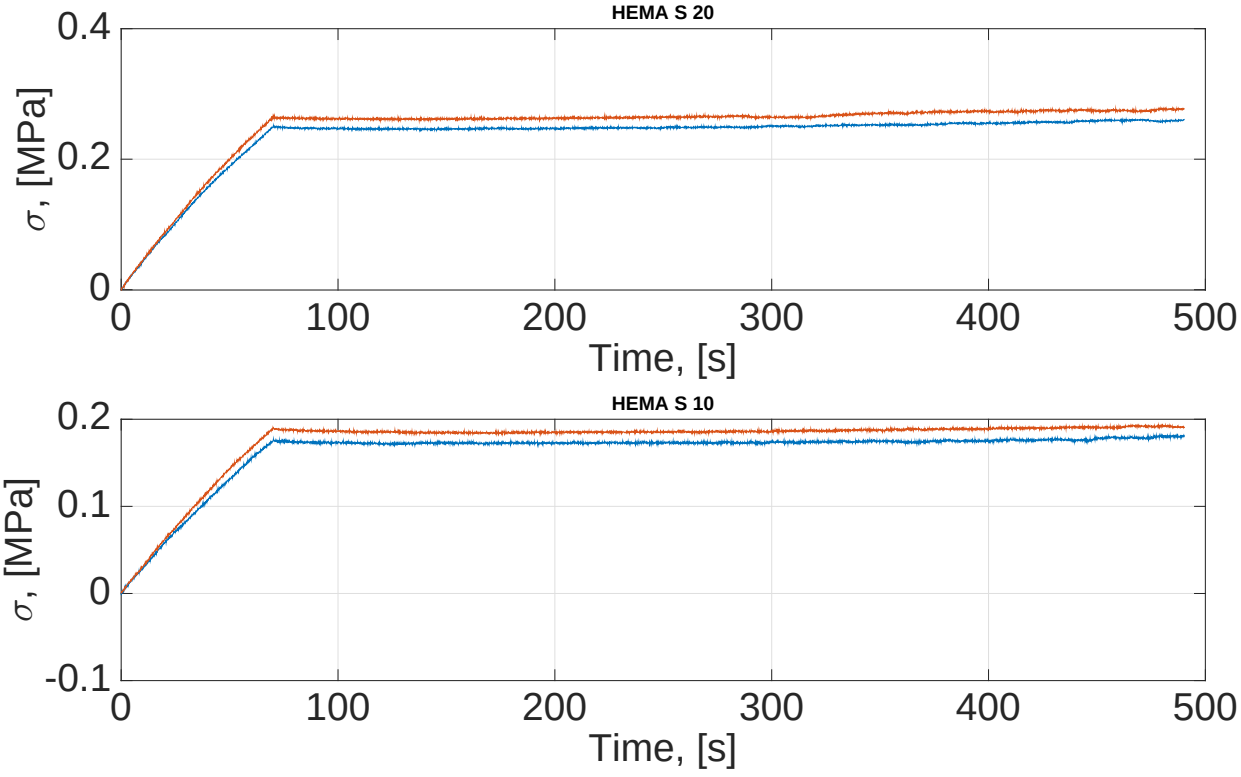

Fig. B.24 Stress σ versus time on swollen specimens.